

Day-Ahead Electricity Price Forecasting Using Merit-Order Curves Time Series

Guillaume Koechlin^{a,*}, Filippo Bovera^b, Piercesare Secchi^a

^a*MOX, Department of Mathematics, Politecnico di Milano, Piazza Leonardo da Vinci
32, Milano, 20133, MI, Italy*

^b*Department of Energy, Politecnico di Milano, Via Lambruschini
4a, Milano, 20156, MI, Italy*

Abstract

We introduce a general, simple, and computationally efficient framework for predicting day-ahead supply and demand merit-order curves, from which both point and probabilistic electricity price forecasts can be derived. Specifically, we leverage functional principal component analysis to efficiently represent a pair of supply and demand curves in a low-dimensional vector space and employ regularized vector autoregressive models for their prediction. We conduct a rigorous empirical comparison of price forecasting performance between the proposed *curve-based* model, i.e., derived from predicted merit-order curves, and state-of-the-art *price-based* models that directly forecast the clearing price, using data from the Italian day-ahead market over the 2023–2024 period. Our results show that the proposed curve-based approach significantly improves both point and probabilistic price forecasting accuracy relative to price-based approaches, with average gains of approximately 5%, and improvements of up to 10% during mid-day hours, when prices occasionally drop due to high renewable generation and low demand.

Keywords:

electricity price forecasting, day-ahead market, merit-order curves, functional data analysis

*Corresponding author

Email address: guillaume.koechlin@polimi.it (Guillaume Koechlin)

1. Introduction

1.1. Context

The rising integration of non-programmable renewable energy sources and the growing uncertainty surrounding fossil fuel supply have made electricity markets more volatile and difficult to forecast. As a result, the development of sophisticated and reliable market forecasting tools has become even more essential for all actors of the electric power industry.

Most wholesale electricity trading in Europe takes place on day-ahead markets, where producers and retailers exchange power one day before delivery. These markets generally operate under a double uniform-price (pay-as-clear) auction mechanism, where the intersection of the supply and demand *merit-order curves* sets the market clearing price for all accepted offers and bids. These curves are formed from the aggregation of individual supply offers and demand bids following the merit order, i.e. increasing price for supply and decreasing price for demand (Fig. 1). Offers (or bids) priced below (resp. above) the clearing price are accepted¹ while the remainder are rejected. For market participants, accurately estimating the clearing price is therefore sufficient to anticipate whether an offer/bid will be accepted and at which price.

Because of this single-price property, a large body of research has focused on forecasting the day-ahead clearing price itself, a discipline known as *electricity price forecasting* (EPF). The consensus is that data-driven approaches based on historical prices tend to outperform *fundamental* (or structural) ones which try to model exact market mechanisms, especially for short-term hourly price forecasting (Weron, 2014). In particular, a highly competitive day-ahead EPF benchmark based on regularized autoregressive models and feedforward neural networks was consolidated by Lago et al. (2021). This framework is still state-of-the-art and has been widely employed in recent studies (Olivares et al., 2023; Lipiecki et al., 2024; O'Connor et al., 2025; Cerasa and Zani, 2025).

Nevertheless, the problem of forecasting the entire merit-order curves underlying price formation is gaining momentum in the academic community (Petropoulos et al., 2022). The seminal work of Ziel and Steinert (2016) demonstrated the capacity of "data-driven fundamental" approaches based

¹The intersection point may split a supply offer or demand bid which in that case would be partially accepted

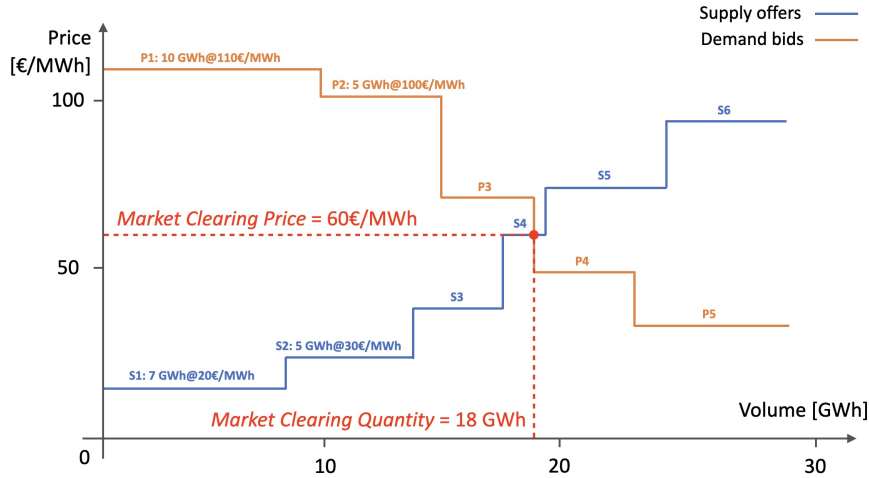


Figure 1: Example an electricity spot market clearing from the supply (in blue) and demand (in orange) merit-order curves.

on historical auction data and their potential for generating competitive clearing price forecasts. Forecasting entire curves offers several advantages. For participants with market power, it enables precise quantification of how marginal changes in offers may influence the clearing price and allows realistic market simulations from which optimal bidding strategies can be derived (Pelagatti, 2013). For price-takers and other actors exposed to the day-ahead price, curve-based models offers a more comprehensive view of market results, enhances the interpretability of price predictions, and may improve the quantification of price predictions' uncertainty². Additionally, complex nonlinear dynamics observed at the price level may become more tractable when modeled at the curve level.

Despite a growing number of contributions, an essential question remains unanswered: Are merit-order curves forecasting models competitive with state-of-the-art price-centric EPF models in terms of clearing price prediction accuracy?

In this context, this work has two main objectives:

1. Introduce a general, simple, and computationally efficient framework for predicting day-ahead supply and demand merit-order curves, from

²This latter aspect is investigated in this paper.

which both point and probabilistic clearing price forecasts can be derived.

2. Rigorously compare, in accordance with best practices established by Lago et al. (2021), the clearing price forecasting performance of *curve-based* models, i.e. derived from merit-order curves predictions, with that of state-of-the-art *price-based* models, which directly model the clearing price.

Our framework builds on Ziel and Steinert (2016) but eliminates the need for curves discretization by preserving their functional form. Specifically, we leverage functional principal component analysis to efficiently represent a pair of supply and demand curves in a vector space and employ regularized vector autoregressive models inspired by EPF literature for their prediction. We compare this functional approach with the original method of Ziel and Steinert and top-performing price-based point and probabilistic EPF models, on the Italian day-ahead market (GME), during the 2023-2024 period.

The remainder of this paper is structured as follows: section 2 reviews previous contributions, section 3 presents the knowledge gap addressed by this work, section 4 details the forecasting and testing methodology, section 5 describes the dataset, section 6 presents and discusses the empirical results, and section 7 provides concluding remarks.

2. A thematic review of prior work

Table 1 provides an overview of contributions on the topic. Rather than providing a linear and descriptive review, we organize it according to several key aspects that we believe are central to the merit-order curve forecasting problem.

2.1. Handling the infinite dimensionality

A central aspect of the problem regards the fact that merit-order curves are essentially infinite-dimensional functional objects, in the sense that they represent quantities that vary over a continuum. It is therefore necessary to consider either an appropriate statistical framework, e.g. functional data analysis (Ramsay and Silverman, 2005; Ferraty and Vieu, 2006) or a finite-dimension representation of the curves to which classic multivariate time series methods can be applied.

Within the functional approach, several generalizations of the autoregressive (AR) models (Box et al., 1994) to the functional setting have been used: Functional AR (FAR) models (Canale and Vantini, 2016; Soloviova and Vargiolu, 2021; Li et al., 2025), functional SARMA (Mestre et al., 2020) and nonparametric FAR (NPFAR) models (Shah and Lisi, 2020). Methodological reference on functional time series include Bosq (2000) and Hörmann and Kokoszka (2012). The advantage of functional approaches, beyond elegantly tackling the problem from a mathematical standpoint, is that they avoid the information loss inherent in finite dimension representations. Their main drawback, however, lies in the limited theoretical development and the lack of efficient, easy-to-use, open-access implementations of the models proposed in the literature (Aue et al., 2015).

Aside of the functional framework, there are essentially three strategies to address the dimensionality problem: discretization, parametrization and dimensionality reduction. For all three, the overall workflow is similar: (i) Transform the curves into a finite-dimension vector form, (ii) Forecast this vector using multivariate methods, and (iii) Invert the transformation to recover the predicted curves.

Although any software ultimately relies on discrete representations, we refer to the *discretization* approach when the vector representation consists of curve evaluations over a grid of reasonable size (no more than a few dozen points), enabling multivariate modeling. The functional form is then recovered using a chosen interpolation method. This strategy was adopted in the seminal work of Ziel and Steinert (2016) and its extensions in Kulakov (2020) and Ghelasi and Ziel (2024). *Parametrization* refers to methods that assume a parametric form (e.g. linear, logarithmic or polynomial) for the curves, with the finite-dimensional representation given by the fitted parameters; see for instance Yıldırım et al. (2023) and Ciarreta et al. (2023). Finally, *dimensionality reduction* refers to approaches where the finite-dimension representation is obtained by means of a low-rank approximation of the data through standard matrix factorization techniques (Guo et al., 2021; Tang et al., 2024), neural networks (Sinha and Lucheroni, 2025) or functional PCA (Pelagatti, 2013; Li et al., 2025).

Functional PCA (FPCA) is a well-known, simple, and effective method for forecasting functional time series (Hyndman and Shahid Ullah, 2007; Hyndman and Shang, 2009; Shang, 2013; Aue et al., 2015). It is therefore a natural choice for a benchmark framework. Further arguments supporting this choice are provided in section 4.2.

Work	Market	Model typology	Dim. reduction	Curve form	Monotonicity constraint	Demand side	Joint prediction	Price forecasting	Probabilistic forecasting
Pelagatti (2013)	GME	VARX	PCA	Inverse	Built-in				
Ziel and Steinert (2016)	EPEX-DE	VARX	Discretization	Inverse	Built-in*	✓	✓	✓	✓
Canale and Vantini (2016)	GME (Gas market)	Functional	✗	Original	Built-in	✓	✓	✓	
Mestre et al. (2020)	GME	Functional	✗	Inverse	Post-processing				
Kulakov (2020)	EPEX-DE	VARX	Discretization	Inverse	Built-in*	✓	✓	✓	
Shah and Lisi (2020)	GME	Functional	✗	Original	✗	✓		✓	✓
Guo et al. (2021)	MISO	Neural Network	PCA	Original	✗				
Soloviova and Vargiolu (2021)	GME	Functional	✗	Original	Built-in*	✓		✓	
Yildirim et al. (2023)	EPIAS	State-space	Parametrization	Inverse	✗				
Ciarreta et al. (2023)	OMIE	VARX	Parametrization	Original	✗	✓	✓	✓	
Tang et al. (2024)	ANEM	Neural Network	PCA, NMF, SDL	Original	✗				
Vivó and Alonso (2024)	OMIE (Intraday market)	Neural Network	✗	Inverse	Post-processing				
Ghelasi and Ziel (2024)	EPEX-DE	VARX	Discretization	Inverse	Built-in*	✓	✓		
Li et al. (2024)	ANEM, OMIE, PJM	k-NN	✗	Inverse	Built-in				
Ghelasi and Ziel (2025)	EPEX-DE	Fundamental	✗	Original	Built-in			✓	
Sinha and Lucheroni (2025)	GME	Neural Network	Autoencoder	Original	Post-processing	✓			
Li et al. (2025)	OMIE	ARIMA, Functional	FPCA	Inverse	Post-processing	✓		✓	

Table 1: Tabular view of (main) previous works addressing supply & demand curves forecasting, sorted by publication year. *The monotonicity constraint is not exactly enforced in this case but may be respected by the predictions in practice.

2.2. Modeling the original vs inverse curve

Being a monotone step-function, a merit-order curve $P(q)$ expressing price as a function of quantity admits an inverse $Q(p)$ expressing quantity as a function of price which is also a monotone step function. These are just two different functional representations of the same data object, and one can easily switch from one representation to an other. Interestingly, a large number of contributions work with the inverse form Q – offering little discussion on the reasons behind this choice – though there is no clear consensus on what is the best representation strategy between the two forms. However, as we will see in section 4.1, the inverse form has a more natural mathematical definition and offers a convenient perspective on the main source of curves variability.

2.3. Addressing the monotonicity constraint

Merit-order curves are by definition monotone, increasing for supply and decreasing for demand and this must be ideally respected for predictions. To enforce this constraint, two strategies appear in the literature:

The first is to transform the curves to work in a space of unconstrained functions, usually achieved applying a composition of a logarithmic and differential operator on the smoothed curves (Pelagatti, 2013; Canale and Vantini, 2016), work with first-order differences over a discretization grid (Ziel and Steinert, 2016; Kulakov, 2020; Ghelasi and Ziel, 2024) or assuming a

monotone parametric form (Soloviova and Vargiolu, 2021; Ciarreta et al., 2023; Ghelasi and Ziel, 2025). Note that works considering the two latter approaches do not exactly enforce the monotonicity constraint as the vector representation – either first-order differences or parametric coefficients – components sign is not constrained in the prediction process. It doesn’t seem however to be an issue in practice.

The second is to post-process the predictions, for instance by taking the predicted curve’s nearest neighbor in the training set (Sinha and Lucheroni, 2025; Li et al., 2025) or applying a correction re-establishing monotonicity in the predicted curve (Mestre et al., 2020; Vivó and Alonso, 2024).

In our case, rather than working in the constrained functional framework, although appealing from a mathematical point of view, we adopt the post-processing approach as the log-differential transformation was found to introduce excessive noise in the FPCA during preliminary experiments.

2.4. Dealing with the step-like characteristic

Merit-order curves are step functions whose step heights and widths vary across both the domain and time. Most studies, either explicitly or implicitly, work with continuous or smooth approximations of these curves – a practice we consider appropriate. Nevertheless, this approach has been criticized by several authors (Vivó and Alonso, 2024; Li et al., 2024, 2025; Sinha and Lucheroni, 2025), who therefore develop techniques that preserve the step-like form, particularly for point forecasts. However, this can lead to inconsistent or misguided modeling choices: For instance, Li et al. (2024) use a k -NN algorithm to predict curves with $k = 1$ to avoid the smoothing induced when averaging curves for $k > 1$, hence departing from the usual bias–variance trade-off considerations usually driving the choice of k . Similarly, Li et al. (2025) use a functional basis of constant functions defined on equal-width, disjoint intervals, thereby imposing fixed step widths, which the data do not exhibit.

Beyond offering a more tractable form, working with smooth approximations is theoretically grounded. Indeed, as pointed out by Pelagatti (2013) and Diquigiovanni et al. (2024), step locations (the bid prices) are random; being real-valued, they can be modeled as realizations of a continuous random variable. Consequently the expected value of the curves process is a smooth

function³ and smooth point forecasts – being conditional mean estimators – are therefore appropriate. This hypothesis is easily verified empirically by inspecting the smoothness of pointwise average curves in real merit-order curves datasets.

2.5. Joint prediction of supply and demand

Day-ahead power demand has historically shown little elasticity making the demand merit-order curve look more like a vertical line close to the load forecast than decreasing steps. This point has undoubtedly motivated academic researchers to focus primarily on the supply side (Pelagatti, 2013; Mestre et al., 2020; Guo et al., 2021; Yildirim et al., 2023; Tang et al., 2024; Li et al., 2025; Ghelasi and Ziel, 2025). However, first, this assumption does not hold for all markets (e.g. EPEX-DE, the German day-ahead market) and second, the increasing penetration of large-scale storage systems together with the growth of demand-side response is likely to increase day-ahead demand elasticity in the next years.

Although any methodology developed for supply curves is trivially applicable to demand curves by considering their opposite (which is a supply-like increasing function) the challenge is to account for the statistical dependence that may exist between the two objects. This point is crucial when the ultimate goal is price forecasting. Among the works that consider both supply and demand curves, only a few propose a method capable of making supply curves depend on past demand curves and vice-versa. A simple yet effective approach (which we adopt in this work) within dimensionality-reduction frameworks is to stack the supply and demand vector representations into a single vector representing the pair, to which multivariate forecasting models can then be applied (Ziel and Steinert, 2016; Ciarreta et al., 2023). This dependence structure is also incorporated by Canale and Vantini (2016) via a bivariate FAR model (a functional extension of a two-dimensional vector AR model) applied directly to the supply–demand function pair. A notable conclusion from their study is that modeling this dependence is indeed essential for achieving the best predictive performance.

2.6. Curves forecast evaluation and clearing price forecasting

A final crucial point regards the way merit-order curves forecasts are evaluated, since not all curves portions carry the same importance. Indeed,

³Further arguments are provided in section 4.2.

in a pay-as-clear auction, the bid price doesn't matter so much as long as it is estimated to fall either below, above or around the market clearing price. As a result, as we move further from the clearing quantity, bid prices may be subject to an arbitrary variability which is irrelevant from an economic point of view. For instance, market participants with variable renewable energy assets may place bids either at $-500\text{€}/\text{MWh}$ ⁴ or $0\text{€}/\text{MWh}$, while still being certain to be cleared if the market clearing price never falls below $10\text{€}/\text{MWh}$. This variability is likely to be hard to capture and does not reflect variability in market outcomes.

A simple way to address this issue, adopted in several works, is to restrict the supply-demand curves pair to the narrowest domain (possibly with some margin) containing all historic intersections, i.e. clearing price-quantity points (Mestre et al., 2020; Shah and Lisi, 2020; Soloviova and Vargiolu, 2021). This is the approach we follow in this work. Since the conditional distribution of the clearing price exhibits smaller temporal variations than that of the clearing quantity – which has lower uncertainty and closely follows daily demand patterns, this approach is likely to be more effective at discarding low-significance bids when curves are represented in their inverse $Q(p)$ form. Another possible approach is to "clip" bid prices within a conservative range of plausible clearing prices, as done by Guo et al. (2021) and Tang et al. (2024). Alternative weighting-based evaluation methods have also been proposed, based on the distribution of bid prices (Vivó and Alonso, 2024; Li et al., 2024) or clearing prices (Tang et al., 2024). Their main drawback is that results tend to be highly sensitive to the chosen weighting scheme.

Finally, a desirable property of supply and demand curves forecasts is their ability to yield accurate clearing price predictions, and they must be evaluated accordingly. As shown in Table 1, most works addressing both supply and demand curves forecasting tested their ability to produce accurate price forecasts, but rarely following the EPF best practices established in Lago et al. (2021).

3. Literature gap and contributions

3.1. Merit-order curves forecasting benchmark

As there are very few direct and fair comparisons between the different merit-order curves forecasting approaches proposed in the literature, and no

⁴The minimum bidding price in European markets.

shared guidelines or best practices for performance evaluation as in EPF, understanding which models work best remains difficult. Moreover, only a small number of papers provide indicative algorithms running times, preventing a clear assessment of their performance/efficiency trade-off.

Ziel and Steinert (2016) were the first to propose a method addressing all aspects of the problem. Their framework is simple, general enough to be applied across different markets, computationally efficient, and relatively easy-to-implement. Yet, aside from a few direct extensions (Kulakov, 2020; Ghelasi and Ziel, 2024) and despite a large number of subsequent contributions, no alternative method has been conclusively shown to outperform the original approach of Ziel and Steinert. Their model therefore remains state-of-the-art and a natural – if not necessary – benchmark for comparison. We identified only one study, Yildirim et al. (2023), that provides a direct comparison of forecast accuracy for supply curves. Their results suggest that their method and that of Ziel and Steinert perform similarly. A comparison is also reported in Sinha and Lucheroni (2025), but the authors state that they employed a modified version of Ziel and Steinert’s model without providing further details. Additionally, we are somewhat skeptical of their results as all considered benchmarks – including Ziel and Steinert’s model – are found to perform far worse than a naive method.

This work aims to provide a general, simple, and computationally efficient benchmark framework for day-ahead supply and demand merit-order curves forecasting, from which both point and probabilistic clearing price predictions can be derived. We conduct a rigorous comparison with Ziel and Steinert’s framework and provide an open-access Python implementation⁵ (github.com/gkchln/moc_forecast) to facilitate replication and application to other merit-order curves datasets.

3.2. Comparison with state-of-the-art EPF models for clearing price prediction

As mentioned earlier in the introduction, it remains unclear whether merit-order curves models are capable of yielding state-of-the-art point and probabilistic clearing price forecasting performance. Back in 2016, Ziel and

⁵We also implement the model of Ziel and Steinert (2016), considering the multivariate models described in this paper – very similar to Ziel and Steinert’s original ones – within a shared software architecture.

Steinert showed that their model outperformed existing price-based approaches for point predictions, but this may no longer be the case, as of 2025.

Several works have validated the effectiveness of curve-based models for clearing price point forecasting by comparing them with price-based approaches, but the latter are often too simple and not representative of top-performing EPF methods. Moreover, the rigorous forecasts evaluation rules recommended by Lago et al. (2021), such as daily recalibration, are seldom followed. Besides, none of the post-2021 contributions offer comparison with the benchmark models of Lago et al., despite their availability in an open-access software (`epftoolbox` Python package). Shah and Lisi (2020) compare their curve-based price forecasts only against basic autoregressive models without exogenous covariates – even though such covariates are necessary for achieving top performance (Weron, 2014). A similar observation applies to Soloviova and Vargiolu (2021), Ciarreta et al. (2023) and Li et al. (2025). Ghelasi and Ziel (2025) consider an "expert" autoregressive model including exogenous covariates, but do not incorporate regularized, parameter-rich autoregressive models with cross-hour dependence, despite evidence that these models consistently outperform expert ARX models (Ziel and Weron, 2018). For probabilistic forecasting, bootstrap-based Monte Carlo approaches similar to ours were proposed by Ziel and Steinert (2016) and Shah and Lisi (2020), but they were not compared with state-of-the-art probabilistic EPF models.

A rigorous empirical comparison between our curve-based price forecasting approach and state-of-the-art price-based EPF models is conducted in this work. The comparison is restricted to regularized, parameter-rich autoregressive models (Ziel, 2016; Uniejewski et al., 2016; Ziel and Weron, 2018; Lago et al., 2021) as our curves forecasting procedure relies on a direct multivariate extension applied to the curves vector representation. In these experiments, all models share a common regularized *vector* autoregression implementation in Python. For probabilistic forecasting, we compare with quantile regression averaging (Nowotarski and Weron, 2018), conformal prediction (Kath and Ziel, 2021) and isotonic distributional regression (Henzi et al., 2021), using the open-access implementation of Lipiecki et al. (2024).

4. Methodology

4.1. Curves definition

Formally, a merit-order curve represents price as a function of quantity $q \rightarrow P(q)$ and is defined from a set of supply offers (demand bids, respectively) characterized by a price and a quantity $(p_1, q_1), (p_2, q_2), \dots, (p_n, q_n)$ sorted following the merit-order, i.e., increasing order of price $p_1 \leq p_2 \leq \dots \leq p_n$ for the supply curve, decreasing order of price $p_1 \geq p_2 \geq \dots \geq p_n$ for the demand curve. Mathematically, a merit-order curve can be defined as follows:

$$P(q) = p_k, \quad \text{if } \sum_{i=0}^{k-1} q_i \leq q < \sum_{i=0}^k q_i, \quad k = 1, \dots, n$$

where we set $q_0 = 0$, for notational convenience. For supply (or demand), $P(q)$ is said to be the marginal price associated to a total offered (resp. demanded) quantity q .

From the definition we can notice that merit-order curves are non-continuous monotone (increasing for supply and decreasing for demand) step functions. A direct consequence is that $q \rightarrow P(q)$ admits an inverse $p \rightarrow Q(p)$ which is itself a monotone step function. It is interesting to note that this inverse has an easier mathematical notation and interpretation. Indeed, its expression matches (for supply curves) the unnormalized⁶ cumulative distribution function (cdf) of a discrete distribution over the support $\{p_1, \dots, p_n\}$. For demand, the only difference is that it is the reverse cdf (or survival function). Using the superscript (s) for supply and (d) for demand, we have:

$$Q^{(s)}(p) = \sum_{i=1}^n q_i \mathbb{1}_{\{p_i \leq p\}}, \quad Q^{(d)}(p) = \sum_{i=1}^n q_i \mathbb{1}_{\{p_i \geq p\}}$$

That is, $Q(p)$ is the quantity that is offered (or demanded) at a price below (resp. above) p . Note that the definition above does not require the sequence of offers (or bids) to be price-ordered. It is more intuitive to work with the quantity function Q as it represents a more familiar mathematical object than the price function P . The quantity function simply tells us about the total offered quantity and how this offered quantity is distributed on the

⁶Given the q_i 's don't sum to 1.

price domain. It also conveniently changes the perspective on the curves variability which is mainly attributed to their inelastic component: seasonal power demand variations for demand curves and renewable energy sources (RES) generation for supply curves.

From now on, unless otherwise specified, references to supply or demand curves will refer to the quantity function.

4.2. Curves representation

The goal is to model and forecast the time series of curves $Q_1^{(s)}, Q_2^{(s)}, \dots, Q_T^{(s)}$ and $Q_1^{(d)}, Q_2^{(d)}, \dots, Q_T^{(d)}$ over a time period composed of T hourly intervals.

Functional Data Analysis (FDA) is a framework that extends traditional statistical methods to handle data that vary over a continuum, such as curves, surfaces, or other functional forms. Unlike classical approaches that analyze discrete points, FDA treats entire functions as the fundamental unit of analysis. It assumes however that only discrete and noisy samples of continuous functions are observed and therefore the first step of any FDA is to estimate the underlying functions from the data – a process known as *smoothing*.

In our case, things are a bit different: we observe the full functions and these functions are not continuous. Nevertheless, as we saw that the quantity function is expressed as the (unnormalized) cdf of some discrete distribution, with a non-fixed, random support, it may be interpreted as a realization of a Dirichlet process (Ferguson, 1973; Teh, 2011) with a continuous base distribution. The corresponding base distribution has a smooth cdf, which then becomes the natural object of analysis.

In order to forecast functional time series, we follow the guidance of Aue et al. (2015) that recommend the use of *functional principal component analysis* (FPCA) to derive an uncorrelated vector representation of the curves and apply standard multivariate time series forecasting methods to this representation, for finally obtaining a curves forecast using the Karhunen-Loève (KL) expansion (Horváth and Kokoszka, 2012). FPCA is a dimensionality reduction technique for functional data, extending classical PCA to infinite-dimensional spaces. It decomposes a set of observed functions into an orthonormal basis that captures the dominant modes of variations in the data. This decomposition yields the truncated KL expansion:

$$Q_t(p) \approx \bar{Q}(p) + \sum_{k=1}^K \beta_{tk} \xi_k(p)$$

where $\bar{Q}(p)$ is the mean function, $\xi_1(p), \xi_2(p), \dots, \xi_K(p)$ are the first K *functional principal components* (FPCs) and $\beta_{t1}, \beta_{t2}, \dots, \beta_{tK}$ are the *scores* of observation t on the first K FPCs. Intuitively, the FPCs can be seen as specific features common to all curves while the scores are measures of how pronounced are these features in a specific curve. The perfect equality holds when $K = \infty$ but in practice a satisfying approximation can be found with a finite K , typically chosen – as in traditional PCA – as the elbow point of the scree plot or such that the ratio of explained variance surpasses a certain threshold (Johnson and Wichern, 2007).

Since FDA assumes smooth functions, the estimated FPCs should also be smooth functions. This smoothness can be achieved either by incorporating a roughness penalty directly into the FPCA estimation procedure or by pre-smoothing the functional data curves prior to applying FPCA. We adopt the latter approach for computational simplicity, utilizing kernel smoothing with the *Nadaraya-Watson* kernel estimator (Ferraty and Vieu, 2004). The bandwidth parameter of the kernel function, which controls the level of smoothness, is chosen using the generalized cross-validation criterion.

Aue et al. show that a vector autoregressive model of order p – VAR(p) – applied to the K -dimensional vector representation given by the scores on the K first principal components is asymptotically equivalent to a functional autoregressive model (Bosq, 2000) of the same order – FAR(p) – when $K \rightarrow \infty$. Therefore, they argue that forecasting the functional time series by forecasting the vector time series of the FPC scores (given that it provides a satisfying dimensionality reduction) with any multivariate forecasting method – being a VAR model or not – is theoretically justified and is easier than devising complex functional models. Note that the uncorrelation property of the FPC scores has motivated approaches where univariate models are separately fitted to each of the score series (Hyndman and Shahid Ullah, 2007; Hyndman and Shang, 2009). As highlighted by Aue et al. (2015), though it can turn out to be a simple and efficient way to forecast the vector of scores, it has the major drawback of overlooking the cross-correlation that can exist at lags greater than zero, since the FPCA procedure only guarantees that the vectors have no instantaneous (lag 0) correlation.

In our case, we would like to account for possible dependence between the supply and demand curves time series. To do so, we perform FPCA separately for the supply and demand curves and by concatenating the K_s scores for the supply curves with the K_d scores of the demand curve, we get

a $K = K_s + K_d$ -dimensional vector representation $\mathbf{y}_1, \dots, \mathbf{y}_T$ of the paired functional series $(Q_t^{(s)}, Q_t^{(d)})_{t \in \{1, \dots, T\}}$, with

$$\mathbf{y}_t = \left[\beta_{t1}^{(s)}, \beta_{t2}^{(s)}, \dots, \beta_{tK_s}^{(s)}, \beta_{t1}^{(d)}, \beta_{t2}^{(d)}, \dots, \beta_{tK_d}^{(d)} \right]^\top$$

The advantage of working with \mathbf{y}_t is triple: (i) we turn an infinite-dimension problem into an intrinsically finite-dimension one, (ii) we phase out the intrinsic dependence of functional data, (iii) we jointly model the supply and demand processes.

We forecast \mathbf{y}_t with some multivariate forecasting model (detailed in the next section), with possibly a set of exogenous covariates \mathbf{x}_t . We then inverse-transform a h -step-ahead forecast $\hat{\mathbf{y}}_{t+h}$ using the truncated KL expansion to get a forecast for the curves pair $(\hat{Q}_{t+h}^{(s)}, \hat{Q}_{t+h}^{(d)})$.

It can happen that curves predictions are not perfectly monotonic. Though preliminary experiments suggested the occurrence of little deviations only and low impact on clearing price predictions, it is still desirable to respect this structural constraint. To do so, we post-process the curves predictions using isotonic regression with the pool-adjacent violators algorithm (Leeuw et al., 2009). Being a highly efficient $O(n)$ algorithm, it has a negligible impact on computation times.

4.3. Forecasting the curves' vector representation

We consider here the day-ahead forecasting problem, regarding the vector hourly time series as 24 separate daily time series, one for each hour of the day. This is common practice in EPF as the 24 hours of the next day are simultaneously settled the day before. In addition, market dynamics vary a lot depending on the hour of the day, justifying to treat them separately. For a detailed motivation of this choice, the reader can refer to Ziel and Weron (2018). We hence change the time indexing of \mathbf{y}_t to consider the value at day d and hour h , $\mathbf{y}_{d,h}$ and we solve 24 one-step-ahead forecasting problems.

We consider four variants of the popular parameter-rich ARX model estimated with LASSO widely used in the context of electricity price forecasting (Ziel, 2016; Uniejewski et al., 2016; Ziel and Weron, 2018; Lago et al., 2021; Uniejewski, 2024). First this framework was shown to be highly performing for price forecasting and second, it was used in Ziel and Steinert (2016). Specifically, we consider two *univariate* models treating each component of $\mathbf{y}_{d,h}$ separately as suggested by Hyndman and Shang (2009) – the *concurrent*

ARX and the *full* ARX – and two *multivariate* models jointly modeling the vector $\mathbf{y}_{d,h}$, the concurrent VARX and the full VARX. The term "concurrent" means the target variable at hour h is influenced only by past values from the same hour h . Conversely, "full" means the variable is also influenced by past values observed at different hours. The comparison between the univariate and the multivariate approaches allow to test the added value of modeling the cross-dependence between scores while the comparison between the concurrent and full approaches allow to test the added value of modeling the cross-dependence between hours.

The *AR* part refers to the fact that lagged values are used to predict future values. In our case, similarly to state-of-the-art EPF models (Lago et al., 2021) we include lags 1, 2, 3 and 7, considering therefore information up to 7 days before. Additionally, each model has the suffix *X* which means that it makes use of exogenous variables which refer to day d and available on $d - 1$ (i.e., they are known in anticipation or they are themselves one-day-ahead forecasts). This set of r exogenous variables is represented by the r -dimensional vector $\mathbf{x}_{d,h}$. Again, like Lago et al. (2021), we also include lags 1 and 7 of these exogenous variables, and a three-dimensional vector \mathbf{z}_d of dummy variables flagging the day type: Mondays, Working days (from Tuesday to Friday), Saturdays and Holidays (Sundays and bank holidays)⁷.

Finally, still following Lago et al.'s guidance, the L^1 -regularization parameter λ is selected as that minimizing the Akaike information criterion (AIC), exploiting the least angle regression (LARS) algorithm (Efron et al., 2004) for the parameter search. Once λ is selected, the model is estimated using the traditional coordinate descent algorithm (Tibshirani, 1996).

4.3.1. Concurrent ARX (ARX)

The concurrent ARX⁸ models each component $y_{d,h}$ of $\mathbf{y}_{d,h}$ as:

$$y_{d,h} = \phi_{1,h}y_{d-1,h} + \phi_{2,h}y_{d-2,h} + \phi_{3,h}y_{d-3,h} + \phi_{7,h}y_{d-7,h} + \boldsymbol{\beta}_{0,h}^\top \mathbf{x}_{d,h} + \boldsymbol{\beta}_{1,h}^\top \mathbf{x}_{d-1,h} + \boldsymbol{\beta}_{7,h}^\top \mathbf{x}_{d-7,h} + \boldsymbol{\theta}_h^\top \mathbf{z}_d + \epsilon_{d,h} \quad (1)$$

⁷Note this is slightly different from Lago et al. (2021) who consider one dummy for each day of the week but similar to Mestre et al. (2020) and addresses the calendar effects issues raised by Ziel and Steinert (2016).

⁸Note that this model is equivalent to a SARIMAX(3,0,0) × (1,0,0)₇, with the difference that it is estimated with the LASSO and not with maximum likelihood.

where $\phi_{\cdot,h}$ are the autoregressive coefficients and $\beta_{\cdot,h}$ and θ_h are the r -dimensional and 3-dimensional vectors of (lagged) exogenous and dummy variables coefficients, respectively.

4.3.2. Full ARX (fARX)

The full ARX⁹, very similar to its homonym in Uniejewski et al. (2016), models each component $y_{d,h}$ of $\mathbf{y}_{d,h}$ as:

$$y_{d,h} = \sum_{j=1}^{24} \phi_{1,h}^{(j)} y_{d-1,j} + \sum_{j=1}^{24} \phi_{2,h}^{(j)} y_{d-2,j} + \sum_{j=1}^{24} \phi_{3,h}^{(j)} y_{d-3,j} + \sum_{j=1}^{24} \phi_{7,h}^{(j)} y_{d-7,j} \quad (2)$$

$$+ \beta_{0,h}^\top \mathbf{x}_{d,h} + \beta_{1,h}^\top \mathbf{x}_{d-1,h} + \beta_{7,h}^\top \mathbf{x}_{d-7,h} + \theta_h^\top \mathbf{z}_d + \epsilon_{d,h}$$

where $\phi_{\cdot,h}^{(j)}$ is the linear effect of the lagged hour j on the hour h .

4.3.3. Concurrent VARX (VARX)

The concurrent VARX models the full vector $\mathbf{y}_{d,h}$ as:

$$\mathbf{y}_{d,h} = \Phi_{1,h} \mathbf{y}_{d-1,h} + \Phi_{2,h} \mathbf{y}_{d-2,h} + \Phi_{3,h} \mathbf{y}_{d-3,h} + \Phi_{7,h} \mathbf{y}_{d-7,h} \quad (3)$$

$$+ \mathbf{B}_{0,h} \mathbf{x}_{d,h} + \mathbf{B}_{1,h} \mathbf{x}_{d-1,h} + \mathbf{B}_{7,h} \mathbf{x}_{d-7,h} + \Theta_h \mathbf{z}_d + \epsilon_{d,h}$$

Where $\Phi_{\cdot,h}$ are $K \times K$ matrices of autoregressive coefficients and $\mathbf{B}_{\cdot,h}$ and $\Theta_{\cdot,h}$ are the $K \times r$ and $K \times 3$ matrices of (lagged) exogenous and dummy variables coefficients, respectively. Contrarily to the two previous models, we allow for cross-dependence – described by the off-diagonal coefficients of $\Phi_{\cdot,h}$ – between the components of $\mathbf{y}_{d,h}$.

4.3.4. Full VARX (fVARX)

The full VARX models the full vector $\mathbf{y}_{d,h}$ as:

$$\mathbf{y}_{d,h} = \sum_{j=1}^{24} \Phi_{1,h}^{(j)} \mathbf{y}_{d-1,j} + \sum_{j=1}^{24} \Phi_{2,h}^{(j)} \mathbf{y}_{d-2,j} + \sum_{j=1}^{24} \Phi_{3,h}^{(j)} \mathbf{y}_{d-3,j} + \sum_{j=1}^{24} \Phi_{7,h}^{(j)} \mathbf{y}_{d-7,j} \quad (4)$$

$$+ \mathbf{B}_{0,h} \mathbf{x}_{d,h} + \mathbf{B}_{1,h} \mathbf{x}_{d-1,h} + \mathbf{B}_{7,h} \mathbf{x}_{d-7,h} + \Theta_h \mathbf{z}_d + \epsilon_{d,h}$$

⁹Similarly, this model is equivalent to a VARX(7), applied to the 24-dimensional vector $[y_{d,1}, \dots, y_{d,24}]^\top$ – with lags from 4, 5, 6 constrained to be null – with the difference that it is estimated with the LASSO and not with maximum likelihood.

Where we impose the restriction that the off-diagonal terms of $\Phi_{\cdot,h}^{(j)}$ must be zero whenever $j \neq h$, that is, cross-dependence is allowed between hours, but only within the same component¹⁰. This restriction is imposed to have a manageable number of parameters. Indeed, without this condition we would have $4 \times [24 \times K] + 3r + 3 = 96K + 3r + 3$ parameters for each component of $\mathbf{y}_{d,h}$, while with this condition the number of parameters is only $4 \times [23 + K] + 3r + 3 = 4K + 3r + 95$. For instance, for $K = 10$ and $r = 4$, the condition implies 147 parameters instead of 975.

4.4. Clearing price point and probabilistic forecasting

The clearing price *point* prediction \hat{p}_t is simply obtained by determining the zero¹¹ of the function $p \rightarrow \hat{Q}_t^{(d)}(p) - \hat{Q}_t^{(s)}(p)$.

Regarding the *probabilistic* prediction, the goal is to forecast the quantiles of the conditional distribution of the price at day d and hour h given all information available at $d-1$. The strategy we adopt is rather straightforward and based on Monte Carlo simulations:

- (1) Estimate the predictive distribution of \mathbf{y}_t nonparametrically using a residual-based bootstrap on a rolling calibration window
- (2) Simulate a vector $\mathbf{y}_t^{(\text{sim})}$ from that distribution
- (3) Inverse transform $\mathbf{y}_t^{(\text{sim})}$ to obtain $(Q_t^{(s,\text{sim})}, Q_t^{(d,\text{sim})})$
- (4) Find the clearing price $p_t^{(\text{sim})}$
- (5) Repeat (2), (3) and (4) N times
- (6) Take the quantiles of the empirical clearing price distribution \hat{F}_t obtained.

The choice of the calibration window is a classic trade-off as short windows have the advantage of capturing potential non-stationarity and correcting eventual forecasts bias while long windows will allow for a more accurate estimation of the errors distribution. To get "the best of both worlds", we proceed as in Lipiecki et al. (2024): We consider four different window sizes: 28 days (4 weeks), 56 days (8 weeks), 91 days (13 weeks) and 182 days (26 weeks) yielding four cdf estimates $\hat{F}_t^{(28)}$, $\hat{F}_t^{(56)}$, $\hat{F}_t^{(91)}$ and $\hat{F}_t^{(182)}$. We

¹⁰In that sense, "semi-full VARX" could be a more precise denomination but we keep "full VARX" for simplicity.

¹¹Computationally speaking, we take the linear interpolation of the two prices concerned by the sign change.

then compute an ensemble prediction $\hat{F}_t^{(\text{ens})}$ considering *vertical* (probability) averaging (Lichtendahl et al., 2013):

$$\hat{F}_t^{(\text{ens})} = \frac{1}{4} \left(\hat{F}_t^{(28)} + \hat{F}_t^{(56)} + \hat{F}_t^{(91)} + \hat{F}_t^{(182)} \right)$$

Regarding step (1), we estimate the multivariate distribution of the K -dimensional forecast error vector $\boldsymbol{\epsilon}_{d,h} = \mathbf{y}_{d,h} - \hat{\mathbf{y}}_{d,h}$. To robustly estimate this distribution which we assume stationary within the calibration window, we consider hour-dependent variances for the marginals but a shared correlation structure: We assume the errors $\boldsymbol{\epsilon}_{d,h}$ for a given hour h are independent and identically distributed (i.i.d.) according to some K -dimensional distribution $\mathcal{D}(\boldsymbol{\mu}_h, \boldsymbol{\Sigma}_h)$ with mean $\boldsymbol{\mu}_h$ and a covariance matrix $\boldsymbol{\Sigma}_h$ which can be decomposed as follows:

$$\boldsymbol{\Sigma}_h = \mathbf{V}_h^{1/2} \mathbf{R} \mathbf{V}_h^{1/2}$$

where \mathbf{V}_h is the $K \times K$ diagonal matrix containing the hour-specific marginals variances and \mathbf{R} the correlation matrix, assumed identical for all hours. Hence, by bootstrapping the *marginal*-standardized residuals

$$\boldsymbol{\eta}_{d,h} = \hat{\mathbf{V}}_h^{-1/2} (\boldsymbol{\epsilon}_{d,h} - \hat{\boldsymbol{\mu}}_{d,h})$$

across *all hours*, we obtain simulations $\boldsymbol{\eta}^* \sim \hat{\mathcal{D}}(\mathbf{0}, \mathbf{R})$ which can be transformed in simulations of $\boldsymbol{\epsilon}_{d,h}$:

$$\boldsymbol{\epsilon}_{d,h}^{(\text{sim})} = \hat{\boldsymbol{\mu}}_h + \hat{\mathbf{V}}_h^{1/2} \boldsymbol{\eta}^*$$

This modeling choice allows us to account for possible hour-dependent uncertainty without having to estimate 24 distinct distributions.

4.5. Benchmark curves and price forecasting models

4.5.1. Naive model

The naive model (**Naive**) works as follows:

$$\hat{Q}_{d,h}^{\text{naive}} = \begin{cases} Q_{d-7,h} & \text{if } d \text{ corresponds to a Monday, Saturday or Sunday} \\ Q_{d-1,h} & \text{otherwise} \end{cases} \quad (5)$$

4.5.2. Ziel and Steinert (2016)

While our approach differs from that of Ziel and Steinert (2016) regarding the curves vector representation, the multivariate forecasting techniques applied to that representation are essentially the same. For that reason, to guarantee a fair comparison between the two approaches, we apply the models detailed in the previous section to (i) our vector of supply and demand FPCA scores (ii) the vector of supply and demand price class volumes obtained with the method described in Ziel and Steinert (2016). We invite the reader to refer to the authors' paper for a rigorous and detailed description of this procedure (as well as for curves reconstruction), which we refer to as *Ziel-Steinert Transformation (ZST)*, as opposed to our *functional principal component analysis (FPCA)*.

Briefly, **ZST** consists of taking the first-order differences of discrete evaluations of the quantity curve on a specific price grid. This price grid is constructed by defining an equispaced *quantity* (or volume) grid and transforming it into a non-uniform *price* grid via the mean price curve $\bar{P}(q)$. For inverse transformation, the differences are cumulatively summed to recover the discrete values and the continuous curves are reconstructed using interpolation based on the mean quantity curve. Fig. 2 shows an example of a transformed and reconstructed supply-demand curves pair.

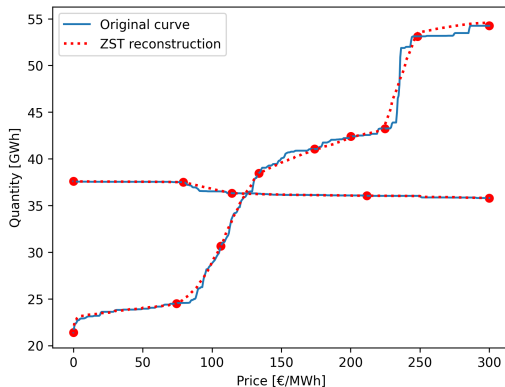


Figure 2: Example of **ZST** reconstruction for a supply-demand curves pair with $K_s = 9$ dimensions for supply and $K_d = 5$ for demand. The vector representation is given by the first-order differences of the y -coordinates of the red dots. The fixed price grid corresponds to their x -coordinates.

4.5.3. Price-based point forecasting models

We consider three benchmark *price-based* clearing price forecasting models: **ARX**, **fARX** and the Lasso-Estimated AutoRegressive model (**LEAR**) of Lago et al. (2021). The first two are already described in the previous section (equations 1 and 2). When both curve-based and price-based models are involved, to distinguish the clearing price forecasting model deriving from the curves model (*curve-based*) from that directly forecasting the price (*price-based*), we prefix the curve-based models with the curves representation used, e.g, **FPCA-ARX** or **ZST-ARX**.

Finally the **LEAR** model is very similar to **fARX** with the difference that it adds cross-hour dependence in the exogenous variables effects and accepts only two of them $\mathbf{x}_{d,h} = [x_{d,h}^1, x_{d,h}^2]^\top$ (usually the load and combined wind-solar generation day-ahead forecasts):

$$\begin{aligned}
 y_{d,h} = & \sum_{j=1}^{24} \phi_{1,h}^{(j)} y_{d-1,j} + \sum_{j=1}^{24} \phi_{2,h}^{(j)} y_{d-2,j} + \sum_{j=1}^{24} \phi_{3,h}^{(j)} y_{d-3,j} + \sum_{j=1}^{24} \phi_{7,h}^{(j)} y_{d-7,j} \\
 & + \sum_{j=1}^{24} \beta_{0,h}^{(j)\top} \mathbf{x}_{d,j} + \sum_{j=1}^{24} \beta_{1,h}^{(j)\top} \mathbf{x}_{d-1,j} + \sum_{j=1}^{24} \beta_{7,h}^{(j)\top} \mathbf{x}_{d-7,j} + \boldsymbol{\theta}_h^\top \mathbf{z}_d + \epsilon_{d,h}
 \end{aligned} \tag{6}$$

As in Lago et al. (2021), for all three models, prices are transformed with median-based scaling and the *area hyperbolic sine* variance stabilizing transformation.

4.5.4. Price-based probabilistic forecasting models

We test the three (price-based) clearing price probabilistic forecasting methods of Lipiecki et al. (2024), using the Julia package `PostForecasts.jl` (Lipiecki and Weron, 2025) developed by the authors: *Quantile Regression Machine* (**QRM**), *Conformal Prediction* (**CP**), *Isotonic Distributional Regression* (**IDR**). We also include the naive *Normal* (**N**) benchmark¹². As these methods are based on post-processing of point predictions, we use the best performing price-based model as a point predictor. For more information, we invite the reader to directly refer to Lipiecki et al. (2024).

¹²Note that differently from Lipiecki et al. (2024) paper, we consider the version which does not suppose zero-mean errors and therefore accounts for potential forecasts bias.

4.6. Forecasts evaluation

4.6.1. Curves forecasts

As suggested in Ramsay and Silverman (2005), we measure curves forecasting accuracy with the *squared correlation function*:

$$R^2(p) = 1 - \frac{\sum_{t=1}^T [\hat{Q}_t(p) - Q_t(p)]^2}{\sum_{t=1}^T [Q_t(p) - \bar{Q}(p)]^2}$$

which represents the proportion of variance explained by the model across the price domain, and the *average squared correlation*:

$$R^2 = \frac{1}{p_{\max} - p_{\min}} \int_{p_{\min}}^{p_{\max}} R^2(p) dp$$

Additionally, to test whether a model significantly outperforms another, we run the *Diebold-Mariano* (DM) test (Diebold and Mariano, 1995) on the L_2 -norm of daily functional forecast errors considering (i) the average L^2 error across the 24 hours (ii) separate tests run on each of the 24 hours¹³. Two one-sided tests are run for each pair of models.

4.6.2. Clearing price forecasts

We evaluate point predictions with the *mean absolute error* (MAE), the *root mean squared error* (RMSE) and the *relative MAE* (rMAE) as defined in Lago et al. (2021).

Price probabilistic predictions are evaluated using the *continuous-ranked probability score* (CRPS):

$$\text{CRPS}(\hat{F}_{P_t}, p_t) = \int_{-\infty}^{\infty} (\hat{F}_{P_t}(x) - \mathbb{1}_{\{p_t \leq x\}})^2 dx \quad (7)$$

where p_t is the realized price at time t and \hat{F}_{P_t} is the estimated conditional cdf we want to evaluate.

Probabilistic forecasting performance is composed of a *reliability* (or calibration) and *sharpness* (or resolution¹⁴) component (Nowotarski and Weron,

¹³Considering daily forecast errors avoids the problem of the strong intraday error auto-correlation, typical in day-ahead price forecasting, which would violate DM tests assumptions (Weron, 2014).

¹⁴The two concepts are equivalent when probabilistic forecasts have perfect reliability.

2018). As any proper scoring rule, the CRPS presents the advantage of simultaneously evaluating both but it can be interesting to understand how models perform on each of these two components. We assess therefore reliability with the *probability integral transform* (Gneiting and Katzfuss, 2014)

$$\text{PIT}_t = \hat{F}_{P_t}(p_t)$$

If p_t is actually drawn from \hat{F}_{P_t} , then PIT_t should be uniformly distributed, which can be verified visually with an histogram (or quantitatively with standard goodness-of-fit statistical tests). Sharpness, when forecasts are reliable, intuitively relates to the capacity of modeling the variability of the response’s uncertainty. A natural way to assess this property is to look at the distribution of a dispersion parameter of the predictive distributions, for instance prediction interval (PI) width or standard deviation. In our experiments, we analyze the joint distribution of the PI width and the magnitude of point forecasts errors to understand if the predicted uncertainty variations are accurate (i.e. larger predicted uncertainty correlates with larger point forecasts errors).

Similarly to the curves forecasts, we perform DM tests for both point and probabilistic forecasts considering average and per-hour daily errors. For point forecasting we consider the absolute (ℓ_1) errors as in Lago et al. (2021) while we use the CRPS, as was done in Nowotarski and Weron (2018), for probabilistic forecasting.

4.7. Daily recalibration

As advised by Lago et al. (2021) and in order to simulate a live forecasting setting, the entire modeling pipeline is recalibrated on a daily basis using a rolling window of 364 days (52 weeks), since ≈ 1 year appears to be the best single-window choice for EPF according to Marcjasz et al. (2018) and Hubicka et al. (2019). This means that for every day d of the testing period:

- (1) We extract the vector representation of the $364 \times 24 = 8744$ curves pairs observed on $d - 1, d - 2, \dots, d - 364$
- (2) We fit the multivariate forecasting model on these vector observations
- (3) We predict the 24 curves vector representations for day d
- (4) We inverse transform the predicted vectors to obtain the 24 curves pairs forecasts

Regarding step (1) this implies that the **FPCA** or **ZST** transformation is re-run from scratch every day. This dynamic "representation learning" procedure is clearly preferable to a time-invariant representation learned on a fixed initial time window but adds a layer of complexity: We must choose the supply and demand dimensions (K_s, K_d) in an automatic manner.

For **FPCA**, we combine the elbow and threshold methods (see section 4.2) by taking the maximum of the two suggested number of FPCs to retain, considering a ratio of 99% for the threshold method. While automating the latter is straightforward, the elbow method relies on a qualitative visual assessment of the scree plot and requires therefore a more sophisticated approach. To automatically find this elbow point in the recalibration procedure, we use the popular knee-point detection method of Satopaa et al. (2011).

For **ZST**, Ziel and Steinert (2016) do not provide discussion on their choice for the number of price classes to consider. Since our goal is to compare the efficiency of the two curves representation strategies, we should ideally match it on a daily basis with the dimension picked by **FPCA**. For simplicity though, we take fixed K_s and K_d equal to their maximum value observed across the **FPCA** recalibration procedure, leaving therefore a slight advantage to **ZST**.

Note that this same daily recalibration procedure applies to the price-based models.

5. Data

5.1. Supply and demand curves

We analyze the supply and demand merit-order curves of the day-ahead electricity market (MGP) of the Italian Power Exchange (IPEX) over the 2023-2024 period. The testing period covers the whole year 2024 (366 days). Note that probabilistic price predictions require at least 182 days of out-of-sample point predictions so the testing period for probabilistic forecasting starts on July 1st, 2024, covering a period of 6 months. The quantity curves are built according to the procedure described in section 4.1, using the `DomandaOfferta` dataset retrieved from the FTP server of Gestore del Mercato Elettrico (GME) – the operator of IPEX – which contains all supply offers and demand bids submitted on the MGP. Three points must be highlighted:

5.1.1. Relaxation of transmission constraints

Around 35% of the time, the country-level economic optimum is not feasible due to transmission capacity constraints, which means that the market cannot be cleared from the country-level supply and demand curves. In this case, GME runs an optimization procedure, known as locational marginal pricing (LMP), which splits the entire country-level market pool in a minimum number of "subpools" of market zones such that, in each subpool, the economic optimum is feasible. As a result, there can be several pairs of supply and demand curves – hence several market clearing prices – for a single hour, one for each subpool. To keep the analysis simple, we did as if the country-level economic optimum was always feasible and built the country-level supply and demand curves for any hour, ignoring the problem of transmission congestion. As a result, the constructed curves reflect the true market clearing 65% of the time, the remaining 35% corresponding to a "virtual" market clearing only. Note the same curves construction procedure was considered in Mestre et al. (2020). The associated market clearing price is what GME calls the *national price without constraints*, and though not always being the exact market price for the different Italian bidding zones, is still a key monitored market indicator.

5.1.2. Market coupling

Italy is integrated into the European electricity market through market coupling with several neighboring countries which are France, Austria, Slovenia and Greece. Market coupling allocates cross-border trading capacity in order to harmonize European prices. It therefore imposes the cross-border exchanges between coupled countries. As a result, the purchased quantity in MGP does not necessarily equal the sold quantity: if Italy imports more than it exports, the (domestic) sold quantity will be lower than the purchased quantity because a part of the demand is already satisfied by the imports. Conversely, if Italy exports more than it imports, the sold quantity will be higher than the purchased quantity because part of the supply must satisfy the exports. As a consequence, the market clearing price is not rigorously at the intersection of the supply and demand curves. However, everything happens as if imports were entering in the supply offers at the minimum price – such that the underlying offer is necessarily accepted – causing a right shift of the price *supply* curve, while foreign exports enter in the demand bids at the maximum price – such that the underlying bid is necessarily accepted – causing a right shift of the price *demand* curve. Therefore by incorporat-

ing the imports and exports in the supply and demand curves, the market clearing is found exactly at the intersection. In our case, the import and export quantities within the scope of market coupling are retrieved from the `MarketCoupling` GME dataset and the difference between imports and exports is added to the quantity supply curve, which is equivalent to adding them separately to both curves (from the point of view of market clearing).

5.1.3. Restriction of the curves domain

A last observation regards the domain on which the quantity curves are analyzed. The entire price domain ranges from -500€ to 3000€ . Obviously, as stressed in the introduction, the part of that domain where the intersection point has negligible chances to occur is of lower interest, may be subject to arbitrary variability that has no impact of the market outcomes and could just add undesired noise in the model. Therefore, we decided to restrict the quantity curves to a price domain that contains at least all prices in the 2023-2024 period with a generous margin: indeed, we restrict the curves to the domain comprised between 0€/MWh and 300€/MWh .

Three example pairs of supply and demand curves of the dataset are showed on Fig. 3

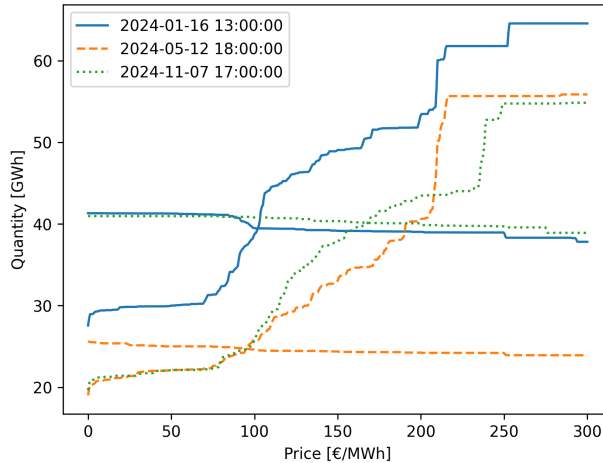


Figure 3: Three example supply-demand curves pairs of during the testing period.

5.2. Exogenous predictors

We collect a total of 4 exogenous variables for both curves and price forecasts which are similar to those of Mestre et al. (2020) and commonly

chosen in EPF:

- *Day-ahead load forecast* (1 variable): Country-level day-ahead load forecast obtained from the ENTSO-E Transparency Platform (ENTSO-E, 2025).
- *Day-ahead net transfer capacities* (2 variables): We consider the import *net transfer capacities* (NTCs) with France and Switzerland obtained from the ENTSO-E transparency platform. These two variables are relevant as Italy (nearly) systematically imports cheaper electricity from France and Switzerland, in the limit of the NTCs. Therefore, variations of the latter directly affect market results – specifically the coupling imports from France and the regular imports (subject to the merit-order) from Switzerland. Note that the other neighboring countries were not considered because of smaller NTCs and the absence of a dominant flow direction.
- *Day-ahead forecast of wind and solar generation* (1 variable): Combined country-level day-ahead forecasts of wind and solar generation obtained from a private data provider (LSEG Data & Analytics, 2025), derived from the European Centre for Medium-Range Weather Forecasts (ECMWF) and Global Forecast System (GFS) weather models.

Note that all these predictors are available at least one hour before the day-ahead market closure at 12:00 and can therefore realistically produce market results forecasts informing trading strategies "in time".

6. Results & Discussion

6.1. Functional Principal Component Analysis

The dynamic number of supply and demand principal components K_s, K_d selected across the test period by our combined elbow-threshold method is pictured on Fig. 4. It turns out this number is rather stable, for both sides with $K_s = 8$ or 9 and $K_d = 4$ or 5 depending on the period.

Fig. 5 shows the dynamic functional principal components across the test period. The stability suggested by the nearly constant number of selected FPCs is confirmed as we can see that each single FPC roughly captures a fixed mode of variation along time. For supply, FPCs subsequent to the fifth start to be noisy with less consistency. Nevertheless, there is a clear shift in

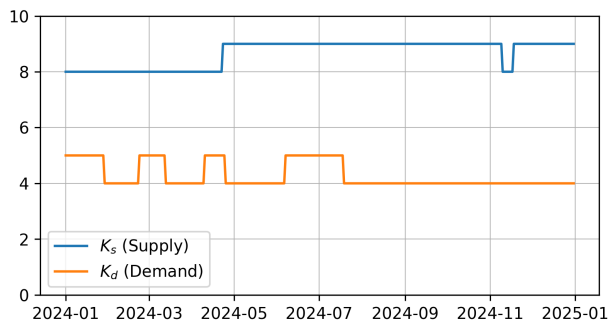


Figure 4: Evolution of the number of functional principal components used for prediction across the testing period

most FPCs, justifying the daily recalibration of FPCA (also motivated by the probable mean shift that is not represented here).

The first five and four supply and demand FPCs can be better interpreted on Fig. 6, which displays the effect a perturbation caused by FPCs on the mean curve for a snapshot of the dynamic FPCA at the middle of the test period. In particular for demand, FPC1 explains the quasi-totality of the variability and concerns the magnitude of the total demanded quantity. The contribution to the total variance beyond FPC1 is negligible. Subsequent FPCs were however selected because the elbow method was in this case less conservative than the threshold method. The additional consideration of their temporal consistency highlighted in 5 suggests their significance and goes against the hypothesis that these FPCs just capture noise. It is likely instead that they could capture the small scale variability in a domain of the curve where the intersection with the supply curve is likely to occur, and that is therefore of interest. For supply, FPC1 measures the overall supply level at any price, while FPC2 contrasts situations where there is higher supply at low price (below 100€/MWh) compared to high price (above 200€/MWh) and vice versa. FPC3 and FPC4 regard the distribution of the prices above (resp. below) 180€/MWh, and similarly contrasts situations when these prices are higher or lower. FPC5 is more difficult to interpret and regards more complex features of the price/volume distribution.

6.2. Curves forecasting

An example of curves (and clearing price) forecast for each of the nine curve-based models can be found in Appendix A (Fig. A.13). The average

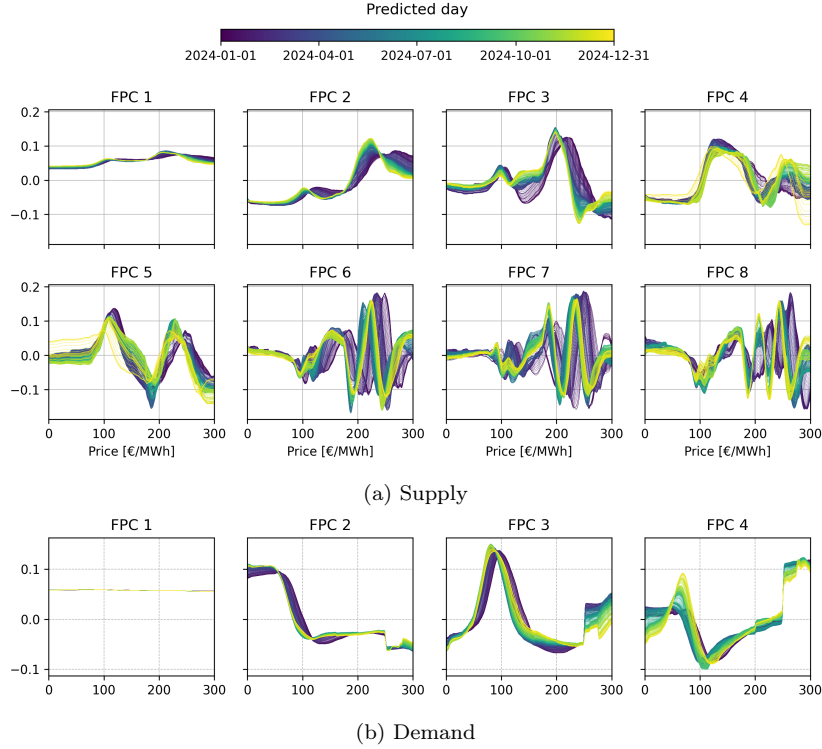


Figure 5: Functional principal components across the test period

squared correlation R^2 and the squared correlation function $R^2(p)$ of the nine curves forecasting models are presented in Table 2 and Fig. 7, respectively. The naive model is clearly outperformed by all the other models for both sides. For demand, all models (except naive) perform almost equally: This is very likely due to the low demand elasticity on the Italian day-ahead market meaning that the quantity demand curve is more or less constant equal to the load forecast – predictor to which all models have access to. Concerning supply, the FPCA representation (**FPCA**) clearly outperforms that of Ziel and Steinert (2016) (**ZST**), while the selected variant of the multivariate forecasting model does not show much impact, especially for **FPCA**. Looking at the entire squared correlation curve, we notice the performance drop of **ZST** models in the high prices range, which partly explains their lower average R^2 .

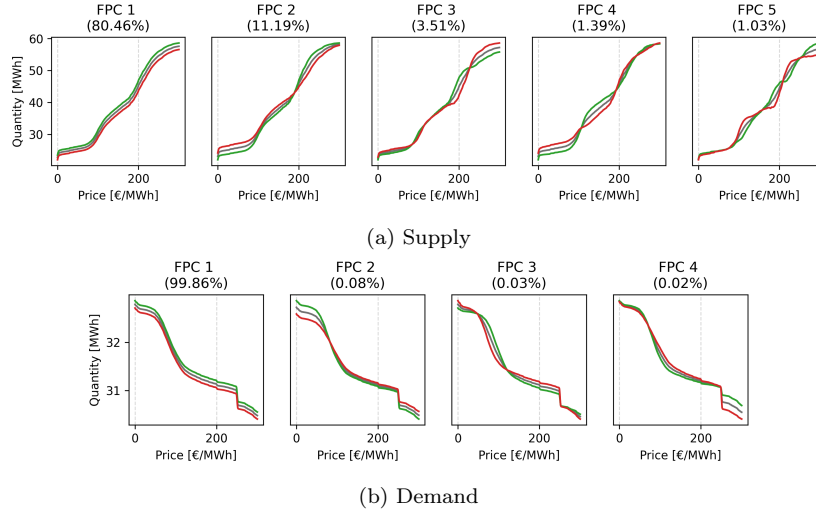


Figure 6: Visualization of the effects of the first 5 (for supply) and 4 (for demand) functional principal components (FPCs) on the mean curve (in grey) estimated for prediction of 2024-07-01. The green curve corresponds to mean curve to which a multiple (20 for supply and 1 for demand) of the FPC is added, while the red curve corresponds to the mean curve to which a multiple of the FPC is subtracted. The number in parenthesis above each plot is the proportion of variance explained by the FPC.

6.3. Clearing price forecast

The global clearing price forecasting performance is reported on Table 3 with the associated DM tests in Fig. 8a, for the four *price-based* and eight *curve-based* models. All models perform well compared to the naive approach. The DM tests reveal that all **ZST** models are significantly outperformed by all **FPCA**, regardless of the multivariate model variant considered. Besides, none of **ZST** models significantly outperform any of the price-based models, while all of them but one are significantly outperformed by at least one of the price-based models. The **FPCA** curve-based models instead are the best performers as all of them significantly beat all **ZST** and price-based approaches¹⁵. A key result is that the consideration of the cross-scores dependence (**VARX** models) appear to have a significant (positive) impact while the cross-hour dependence (**full** models) does not show any improvement, whether it be for **ZST** or **FPCA**. Instead, for the price-based models, the cross-hour dependence is necessary to reach top performance.

¹⁵At the 5% level except for the univariate FPCA models vs **fARX** for which it is 10%.

	R^2_{supply}	R^2_{demand}
Naive	0.755	0.908
ZST-ARX	0.853	0.991
ZST-fARX	0.847	0.992
ZST-VARX	0.869	0.990
ZST-fVARX	0.860	0.991
FPCA-ARX	0.912	0.991
FPCA-fARX	0.916	0.992
FPCA-VARX	0.913	0.991
FPCA-fVARX	0.915	0.992

Table 2: Curves forecasting performance measured with the average squared correlation.

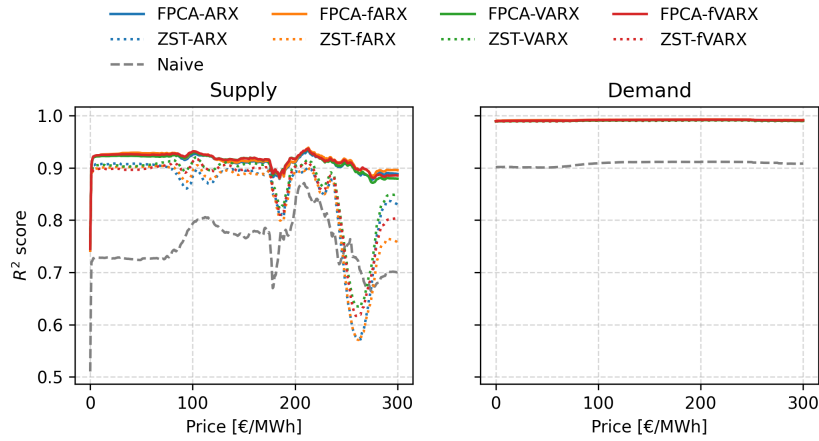


Figure 7: Performance of curves prediction measured with the squared correlation function $R^2(p)$

Note the large performance gap between **ZST-ARX** and **ZST-VARX** (almost 1 €/MWh) compared to that observed between **FPCA-ARX** and **FPCA-VARX** (around 0.20€/MWh). This observation confirms a priori beliefs on the efficiency of the functional vs discretization representation method for capturing the statistical dependence that may exist between different portions of curves domain.

Fig. 9 shows the hour-level performance of each category’s best model: **fARX** for price-based, **ZST-VARX** for **ZST** curve-based and **FPCA-VARX** for **FPCA** curve-based, while DM tests performed at the hour-level can be found in Fig. 8b. We understand that the **FPCA** model performs

		MAE	rMAE	RMSE
<i>price-based</i>	Naive	11.34	1.000	17.24
	ARX	8.35	0.736	11.89
	fARX	7.97	0.703	11.37
	LEAR	8.24	0.727	11.65
<i>curve-based</i>	ZST-ARX	9.12	0.804	13.10
	ZST-fARX	8.91	0.786	12.92
	ZST-VARX	8.22	0.725	11.82
	ZST-fVARX	8.52	0.751	12.31
	FPCA-ARX	7.79	0.687	11.52
	FPCA-fARX	7.80	0.688	11.61
	FPCA-VARX	7.61	0.671	11.19
	FPCA-fVARX	7.66	0.676	11.51

Table 3: Clearing price prediction performance

particularly well around mid-day, between 12 and 16, matching the period of simultaneous low-demand and high RES generation occasioning price drops, while the price-based model shows a slight advantage – confirmed by DM tests – during the night.

To understand more precisely the difference between the price-based and curve-based forecasts and visualise performance across the price range, we can refer to Fig. 10 where predicted prices are plotted against true prices for each model. Without much surprise, largest errors occur at the tails of the distribution, particularly on the left-side i.e. for prices below 100€/MWh. Note the two opposed biases between price-based and **FPCA** curve-based models as the first systematically overestimate prices below ≈ 50 €/MWh while the second tend to underestimate them. This observation suggests that considering an ensemble of price-based and curve-based models is likely to provide significant improvements.

6.4. Price probabilistic forecasting

The average CRPS of the clearing price probabilistic forecasting models are reported in Table 4 with the associated DM tests in Fig. 12. Again, all models outperform the naive strategy but the curve-based models based on **ZST** representation do not perform well compared to that based on **FPCA** and price-based models. While **FPCA** curve-based models perform globally better than price-based approaches, **fARX-QRM** strongly benefits from

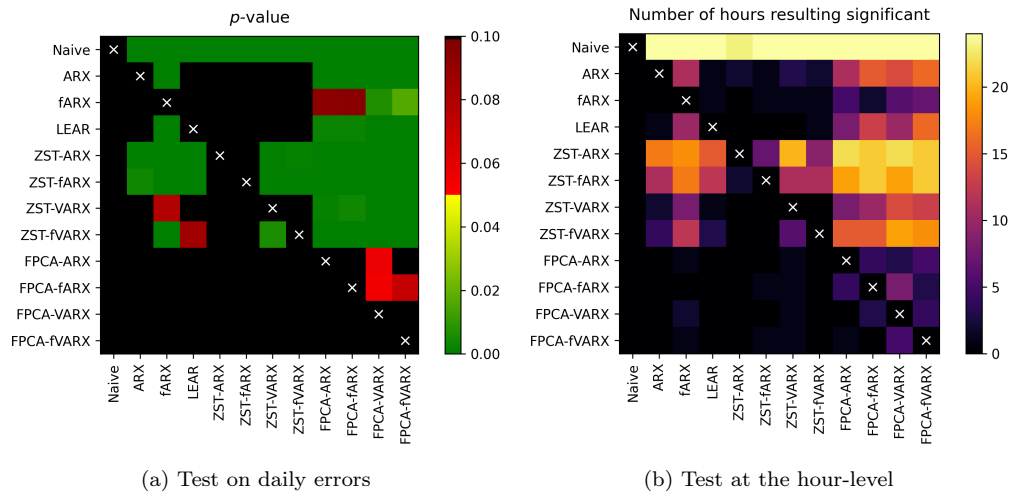


Figure 8: Results of the Diebold-Mariano test for the difference in price *point* forecasting performance performed (a) on average daily errors (b) at the hour level. The alternative hypothesis is that models on the x -axis outperform those on the y -axis (one-sided test).

the ensemble averaging effect and only two of the curve-based models significantly outperform it at the 10% level regarding daily average errors. The top performers for point forecasting were the multivariate **FPCA** models, but for probabilistic forecasting, results suggest a slight advantage for univariate versions.

Fig. 11 shows the hour-level average CRPS of the best models of each category. As for point forecasting, the best curve-based model performs better in the early afternoon between 12 and 16 than the price-based approach. The performances are nearly equal for the rest of the day.

Looking at the calibration and resolution components (Fig. B.14 and B.15 left in Appendix B), we notice the poor reliability of the curve-based **ZST** and price-based **fARX-IDR** models. The first is strongly over-dispersed while the tails of the second are too light. **fARX-N** forecasts are reliable but show a poor resolution. The other models show comparable calibration – with a slight under-dispersion and clear skew towards lower prices – but heterogeneous resolutions: low for **fARX-CP**, intermediate for **fARX-QRM** and higher for **FPCA** models.

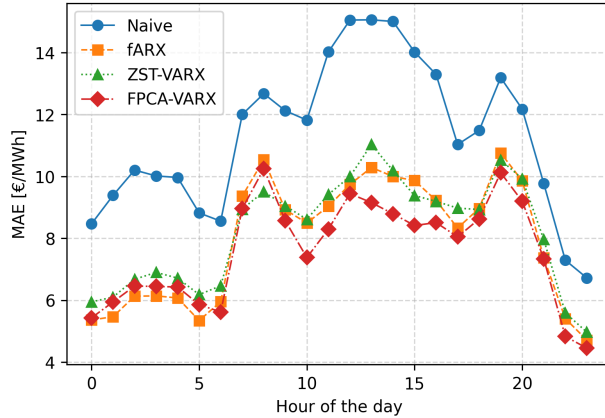


Figure 9: Mean absolute error of the three best performing models within each category (*price-based* and *curve-based* with either Ziel and Steinert (2016) or FPCA representation) for each hour of the day

6.5. Computational efficiency

The computational time requirements for point and probabilistic forecasting models (Table 5 and 6) were evaluated on an Apple M2 Pro chip with a 12-core CPU and 16GB of RAM. Note that the **ARX** model could be made more efficient by parallelizing model fits across hours or vector components. The remaining models benefit from NumPy’s built-in multithreading for large matrix operations and therefore execute in a multicore fashion.

Price-based point forecasting models are definitely faster as they require fitting only 24 individual regression models, compared with the $24 \times K$ fits needed for curve-based models. Nevertheless, the overall computational cost remains low across all approaches. For probabilistic forecasting, the price-based normal (**N**), conformal prediction (**CP**), and isotonic distributional regression (**IDR**) models are highly efficient, whereas the quantile regression machine (**QRM**) is substantially more expensive. However, **QRM** is the only price-based method that was found competitive against curve-based models, which exhibit comparable computational efficiency.

7. Conclusion

This work introduced a general framework for forecasting day-ahead merit-order curves, leveraging functional principal component analysis to efficiently represent a pair of supply and demand curves in a vector space and employing

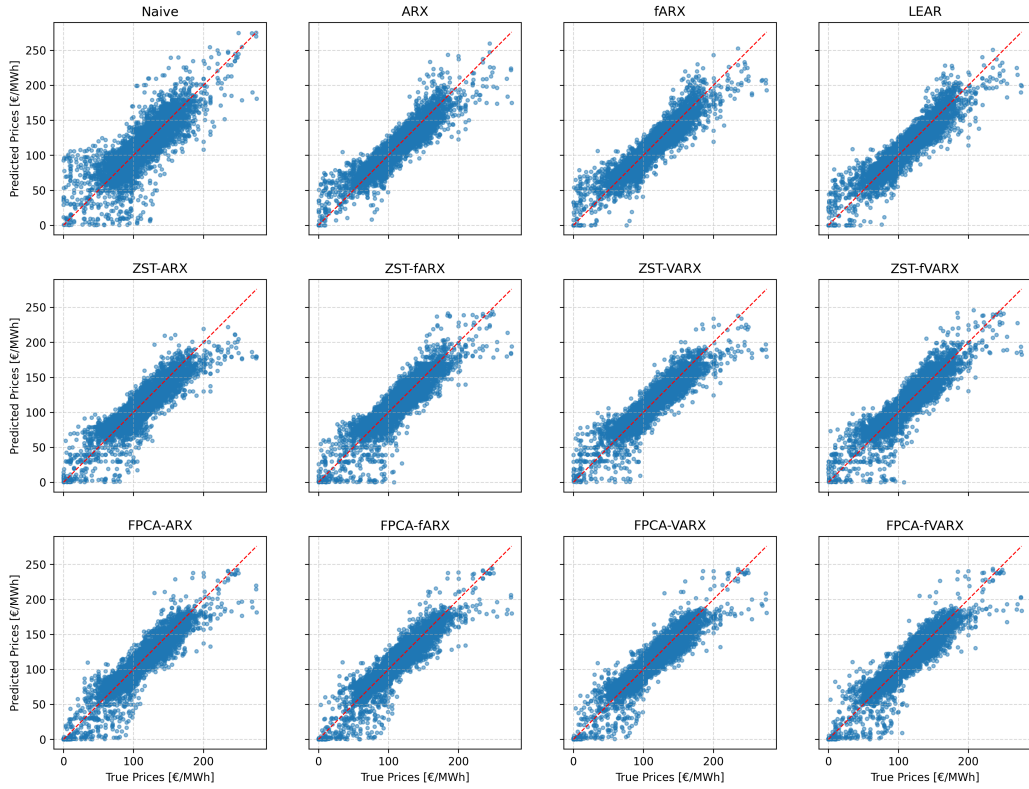


Figure 10: Predicted vs actual clearing prices for all price-based and curve-based models. Each point represents one of the 8744 hourly observations in the test period. The dashed red line is the $y = x$ line.

regularized vector autoregressive models for their prediction. The application to the Italian day-ahead market during the 2023-2024 period not only demonstrated the method’s effectiveness in forecasting merit-order curves but also in producing highly accurate clearing price point and probabilistic forecasts.

We tested four variations of our model, each treating the hourly time series as 24 independent daily time series – one for each hour – and differing in whether they accounted for (i) cross-dependence between hours and (ii) cross-dependence between components of the vector representation. Our findings indicate that accounting for cross-component dependence slightly improves clearing price forecasting performance, while cross-hour dependence does not yield significant gains.

		28D	56D	91D	182D	Avg.
<i>Price-based</i>	Naive-N	9.294	9.359	9.377	9.284	9.239
	fARX-N	6.214	6.189	6.186	6.207	6.147
	fARX-QRM	6.201	6.111	6.122	6.154	5.968
	fARX-CP	6.151	6.142	6.167	6.183	6.138
	fARX-IDR	6.807	6.663	6.529	6.518	6.347
<i>curve-based</i>	ZST-ARX	7.567	7.413	7.283	7.248	7.182
	ZST-fARX	7.351	7.234	7.121	6.930	7.040
	ZST-VARX	7.188	7.097	7.009	6.711	6.870
	ZST-fVARX	7.278	7.128	7.058	6.858	6.979
	FPCA-ARX	5.776	5.744	5.764	5.778	5.735
	FPCA-fARX	5.761	5.747	5.762	5.796	5.733
	FPCA-VARX	5.847	5.838	5.884	5.841	5.815
	FPCA-fVARX	5.928	5.954	5.975	5.944	5.923

Table 4: Average *Continuous Ranked Probability Score* (CRPS) for probabilistic clearing price forecasting across different calibration windows (in **Days**) and their ensemble obtained through vertical (probability) averaging

Our curve-based model was rigorously compared with that of Ziel and Steinert (2016) – which share the same multivariate forecasting framework and differs only in the curves representation strategy – and state-of-the-art price-based models for clearing price forecasting. The results show that considering a functional principal component representation brings consequent improvements over a discrete representation and that our curve-based model – even in its simplest form – significantly enhances point and probabilistic clearing price forecasting performance, especially around mid-day when price occasionally drops due to high renewable generation and low demand. Specifically, our curve-based model reduces the mean absolute error by 5% and the continuous ranked probability score by 4%. If we restrict the comparison to the 10:00-17:00 hour range, the reduction is of 10% and 7%, respectively.

Additional analyses could examine the effect of alternative curves representations¹⁶, the vector space dimension, the use of a single versus hour-specific representation and the calibration window size on both curves and clearing price forecasting performance. Besides, more complex non-linear models such as feedforward neural networks could be considered to jointly predict the 24-hour score matrix. Finally, the recent switch to 15-min in-

¹⁶Such as the original form $P(q)$ and/or unconstrained forms (c.f. section 2.3).

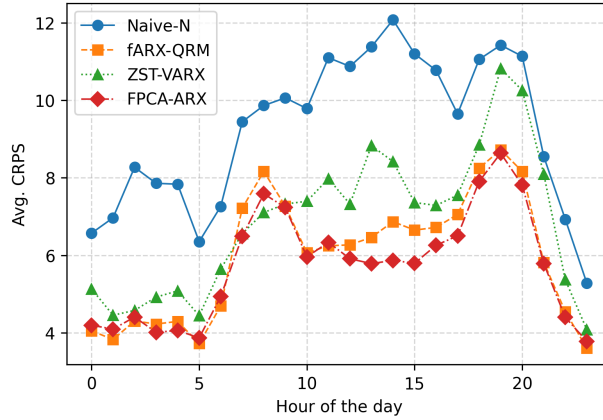


Figure 11: Average CRPS error of the two best performing models within each category, ensemble across the four time windows (*price-based* and *curve-based* with either Ziel and Steinert (2016) or FPCA representation) for each hour of the day.

tervals in European day-ahead markets, making no longer 24 but 96 curves pairs to predict, could justify a functional rather than multivariate perspective to capture intraday dependence. These aspects will be explored in future research.

Acknowledgments

The authors would like to thank Riccardo Barilli and Giulio Caprara of Energy Team S.p.A. for their support in the creation of the dataset used in this analysis and their contribution to the interesting and deep discussions on the topics developed in this paper. This work was funded by Energy Team S.p.A. and MUR, grant Dipartimento di Eccellenza 2023-2027.

Code and data availability

An open-source software implementation of the methods described in this paper, along with the code and data needed to reproduce all numerical results, are available online at https://github.com/gkchln/moc_forecast.

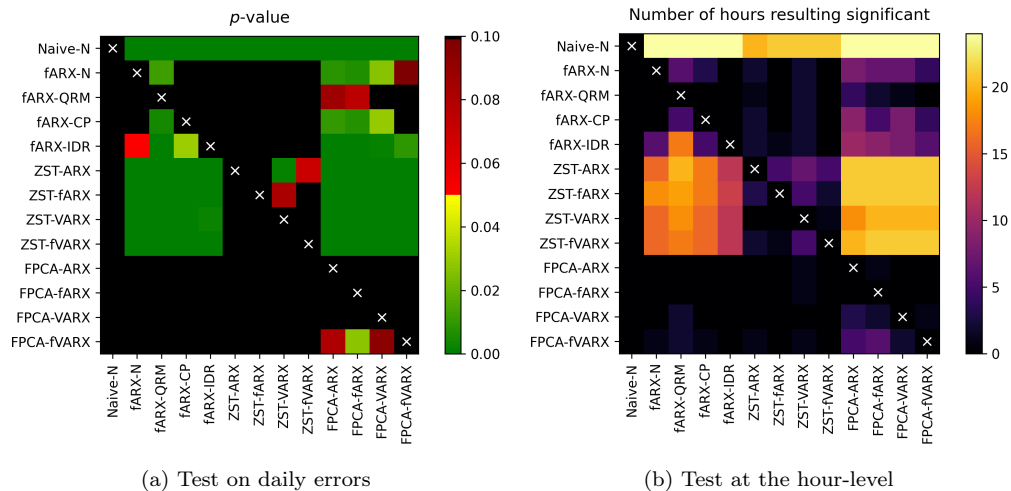


Figure 12: Results of the Diebold-Mariano test for the difference in price *probabilistic* forecasting performance as measured by the CRPS. The ensemble model obtained by averaging the four 28, 56, 91 and 182-days calibration windows is considered. The alternative hypothesis is that models on the x -axis outperform those on the y -axis (one-sided test).

Declaration of generative AI and AI-assisted technologies in the writing process

During the preparation of this work the authors used OpenAI ChatGPT and Google Gemini in order to obtain suggestions for improving writing fluency and clarity. After using this tool/service, the authors reviewed and edited the content as needed and take full responsibility for the content of the published article.

CRedit author statement

Guillaume Koechlin: Conceptualization, Methodology, Software, Writing - Original Draft, Visualization. **Filippo Bovera:** Conceptualization, Methodology, Writing - Review & Editing. **Piercesare Secchi:** Conceptualization, Methodology, Writing - Review & Editing.

References

Aue, A., Norinho, D.D., Hörmann, S., 2015. On the Prediction of Stationary Functional Time Series. *Journal of the American Statistical Association*

	Wall time
ARX	0.2s
fARX	0.6s
LEAR	3s
ZST/FPCA-ARX	2s
ZST/FPCA-fARX	9s
ZST/FPCA-VARX	6s
ZST/FPCA-fVARX	16s

Table 5: Average computational time required for one daily iteration of price *point* forecasting. A daily iteration consists of (i) scaling/transforming the data & fitting the model to the last 364 days (ii) predicting the 24 prices of the next day.

	Wall time
N	<0.1s
QRM	5s
CP	<0.1s
IDR	<0.1s
ZST/FPCA	3s

Table 6: Average computational time required for one daily iteration of price *probabilistic* forecasting using a 182-day calibration window. A daily iteration consists of fitting the probabilistic model to the point forecasts and observed prices on the last 182 days and predicting the 24 x 99 quantiles for the next day.

110, 378–392. URL: <https://doi.org/10.1080/01621459.2014.909317>, doi:10.1080/01621459.2014.909317. publisher: Taylor & Francis
_eprint: <https://doi.org/10.1080/01621459.2014.909317>.

Bosq, D., 2000. Linear Processes in Function Spaces: Theory and Applications. Springer Science & Business Media. Google-Books-ID: lqWEH23nytQC.

Box, G.E.P., Jenkins, G.M., Reinsel, G.C., 1994. Time series analysis: forecasting and control. 3rd ed ed., Prentice Hall, Englewood Cliffs (N.J.).

Canale, A., Vantini, S., 2016. Constrained functional time series: Applications to the Italian gas market. International Journal of Forecasting 32, 1340–1351. URL: <https://www.sciencedirect.com/science/article/pii/S0169207016300620>, doi:10.1016/j.ijforecast.2016.05.002.

- Cerasa, A., Zani, A., 2025. Enhancing electricity price forecasting accuracy: A novel filtering strategy for improved out-of-sample predictions. *Applied Energy* 383, 125357. URL: <https://linkinghub.elsevier.com/retrieve/pii/S030626192500087X>, doi:10.1016/j.apenergy.2025.125357.
- Ciarreta, A., Martinez, B., Nasirov, S., 2023. Forecasting electricity prices using bid data. *International Journal of Forecasting* 39, 1253–1271. URL: <https://www.sciencedirect.com/science/article/pii/S016920702000711>, doi:10.1016/j.ijforecast.2022.05.011.
- Cleveland, W.S., 1979. Robust Locally Weighted Regression and Smoothing Scatterplots. *Journal of the American Statistical Association* 74, 829–836. URL: <http://www.tandfonline.com/doi/abs/10.1080/01621459.1979.10481038>, doi:10.1080/01621459.1979.10481038.
- Diebold, F.X., Mariano, R.S., 1995. Comparing Predictive Accuracy. *Journal of Business & Economic Statistics* 13, 253–263. URL: <https://www.tandfonline.com/doi/abs/10.1080/07350015.1995.10524599>, doi:10.1080/07350015.1995.10524599. publisher: ASA Website _eprint: <https://www.tandfonline.com/doi/pdf/10.1080/07350015.1995.10524599>.
- Diquigiovanni, J., Fontana, M., Vantini, S., 2024. Distribution-Free Prediction Bands for Multivariate Functional Time Series: an Application to the Italian Gas Market. URL: <http://arxiv.org/abs/2107.00527>, doi:10.48550/arXiv.2107.00527. arXiv:2107.00527 [stat].
- Efron, B., Hastie, T., Johnstone, I., Tibshirani, R., 2004. Least angle regression. *The Annals of Statistics* 32, 407–499. URL: <https://projecteuclid.org/journals/annals-of-statistics/volume-32/issue-2/Least-angle-regression/10.1214/009053604000000067.full>, doi:10.1214/009053604000000067. publisher: Institute of Mathematical Statistics.
- ENTSO-E, 2025. ENTSO-E Transparency Platform. URL: <https://transparency.entsoe.eu/>.
- Ferguson, T.S., 1973. A Bayesian Analysis of Some Nonparametric Problems. *The Annals of Statistics* 1. URL: <https://projecteuclid.org/journals/annals-of-statistics/volume-1/issue-2/A-Bayesian-Analysis>

s-of-Some-Nonparametric-Problems/10.1214/aos/1176342360.full,
doi:10.1214/aos/1176342360.

Ferraty, F., Vieu, P., 2004. Nonparametric models for functional data, with application in regression, time series prediction and curve discrimination. *Journal of Nonparametric Statistics* 16, 111–125. URL: <https://doi.org/10.1080/10485250310001622686>, doi:10.1080/10485250310001622686. publisher: Taylor & Francis _eprint: <https://doi.org/10.1080/10485250310001622686>.

Ferraty, F., Vieu, P., 2006. *Nonparametric Functional Data Analysis*. Springer Series in Statistics, Springer New York. URL: <http://link.springer.com/10.1007/0-387-36620-2>, doi:10.1007/0-387-36620-2.

Ghelasi, P., Ziel, F., 2024. Hierarchical forecasting for aggregated curves with an application to day-ahead electricity price auctions. *International Journal of Forecasting* 40, 581–596. URL: <https://www.sciencedirect.com/science/article/pii/S0169207022001479>, doi:10.1016/j.ijforecast.2022.11.004.

Ghelasi, P., Ziel, F., 2025. A data-driven merit order: Learning a fundamental electricity price model. URL: <http://arxiv.org/abs/2501.02963>, doi:10.48550/arXiv.2501.02963. arXiv:2501.02963 [stat].

Gneiting, T., Katzfuss, M., 2014. Probabilistic Forecasting. *Annual Review of Statistics and Its Application* 1, 125–151. URL: <https://www.annualreviews.org/doi/10.1146/annurev-statistics-062713-085831>, doi:10.1146/annurev-statistics-062713-085831.

Guo, H., Chen, Q., Zheng, K., Xia, Q., Kang, C., 2021. Forecast Aggregated Supply Curves in Power Markets Based On LSTM Model. *IEEE Transactions on Power Systems* 36, 5767–5779. URL: <https://ieeexplore.ieee.org/document/9430706>, doi:10.1109/TPWRS.2021.3079923.

Henzi, A., Ziegel, J.F., Gneiting, T., 2021. Isotonic Distributional Regression. *Journal of the Royal Statistical Society Series B: Statistical Methodology* 83, 963–993. URL: <https://academic.oup.com/jrsssb/article/83/5/963/7056107>, doi:10.1111/rssb.12450.

Horváth, L., Kokoszka, P., 2012. *Inference for Functional Data with Applications*. volume 200 of *Springer Series in Statistics*. Springer, New York,

- NY. URL: <https://link.springer.com/10.1007/978-1-4614-3655-3>, doi:10.1007/978-1-4614-3655-3.
- Hubicka, K., Marcjasz, G., Weron, R., 2019. A Note on Averaging Day-Ahead Electricity Price Forecasts Across Calibration Windows. *IEEE Transactions on Sustainable Energy* 10, 321–323. URL: <https://ieeexplore.ieee.org/document/8458131>, doi:10.1109/TSTE.2018.2869557.
- Hyndman, R.J., Shahid Ullah, M., 2007. Robust forecasting of mortality and fertility rates: A functional data approach. *Computational Statistics & Data Analysis* 51, 4942–4956. URL: <https://www.sciencedirect.com/science/article/pii/S0167947306002453>, doi:10.1016/j.csda.2006.07.028.
- Hyndman, R.J., Shang, H.L., 2009. Forecasting functional time series. *Journal of the Korean Statistical Society* 38, 199–211. URL: <https://www.sciencedirect.com/science/article/pii/S1226319209000398>, doi:10.1016/j.jkss.2009.06.002.
- Hörmann, S., Kokoszka, P., 2012. 7 - Functional Time Series, in: Subba Rao, T., Subba Rao, S., Rao, C.R. (Eds.), *Handbook of Statistics*. Elsevier, volume 30 of *Time Series Analysis: Methods and Applications*, pp. 157–186. URL: <https://www.sciencedirect.com/science/article/pii/B9780444538581000077>, doi:10.1016/B978-0-444-53858-1.00007-7.
- Johnson, R.A., Wichern, D.W., 2007. *Applied multivariate statistical analysis*. 6. ed ed., Pearson/Prentice Hall, Upper Saddle River, NJ.
- Kath, C., Ziel, F., 2021. Conformal prediction interval estimation and applications to day-ahead and intraday power markets. *International Journal of Forecasting* 37, 777–799. URL: <https://www.sciencedirect.com/science/article/pii/S0169207020301473>, doi:10.1016/j.ijforecast.2020.09.006.
- Kulakov, S., 2020. X-Model: Further Development and Possible Modifications. *Forecasting* 2, 20–35. URL: <https://www.mdpi.com/2571-9394/2/1/2>, doi:10.3390/forecast2010002. number: 1 Publisher: Multidisciplinary Digital Publishing Institute.

- Lago, J., Marcjasz, G., De Schutter, B., Weron, R., 2021. Forecasting day-ahead electricity prices: A review of state-of-the-art algorithms, best practices and an open-access benchmark. *Applied Energy* 293, 116983. URL: <https://www.sciencedirect.com/science/article/pii/S0306261921004529>, doi:10.1016/j.apenergy.2021.116983.
- Leeuw, J.D., Hornik, K., Mair, P., 2009. Isotone Optimization in *R* : Pool-Adjacent-Violators Algorithm (PAVA) and Active Set Methods. *Journal of Statistical Software* 32. URL: <http://www.jstatsoft.org/v32/i05/>, doi:10.18637/jss.v032.i05.
- Li, Z., Alonso, A.M., Elías, A., Morales, J.M., 2024. Clustering and forecasting of day-ahead electricity supply curves using a market-based distance. *International Journal of Electrical Power & Energy Systems* 158, 109977. URL: <https://www.sciencedirect.com/science/article/pii/S0142061524001984>, doi:10.1016/j.ijepes.2024.109977.
- Li, Z., Alonso, A.M., Pascual, L., 2025. Predicting electricity supply and demand curves with functional data techniques. *International Journal of Electrical Power & Energy Systems* 166, 110561. URL: <https://linkinghub.elsevier.com/retrieve/pii/S0142061525001127>, doi:10.1016/j.ijepes.2025.110561.
- Lichtendahl, K.C., Grushka-Cockayne, Y., Winkler, R.L., 2013. Is It Better to Average Probabilities or Quantiles? *Management Science* 59, 1594–1611. URL: <https://pubsonline.informs.org/doi/10.1287/mnsc.1120.1667>, doi:10.1287/mnsc.1120.1667.
- Lipiecki, A., Uniejewski, B., Weron, R., 2024. Postprocessing of point predictions for probabilistic forecasting of day-ahead electricity prices: The benefits of using isotonic distributional regression. *Energy Economics* 139, 107934. URL: <https://www.sciencedirect.com/science/article/pii/S014098832400642X>, doi:10.1016/j.eneco.2024.107934.
- Lipiecki, A., Weron, R., 2025. PostForecasts.jl: A Julia package for probabilistic forecasting by postprocessing point predictions. *SoftwareX* 31, 102200. URL: <https://linkinghub.elsevier.com/retrieve/pii/S2352711025001670>, doi:10.1016/j.softx.2025.102200.

- LSEG Data & Analytics, 2025. ECMWF/GFS wind and solar generation forecasts for Italy. URL: <https://www.lseg.com/en/data-analytics/financial-data/commodities-data/energy-commodities-pricing>.
- Marcjasz, G., Serafin, T., Weron, R., 2018. Selection of Calibration Windows for Day-Ahead Electricity Price Forecasting. *Energies* 11, 2364. URL: <https://www.mdpi.com/1996-1073/11/9/2364>, doi:10.3390/en11092364. number: 9 Publisher: Multidisciplinary Digital Publishing Institute.
- Mestre, G., Portela, J., Muñoz San Roque, A., Alonso, E., 2020. Forecasting hourly supply curves in the Italian Day-Ahead electricity market with a double-seasonal SARMAHX model. *International Journal of Electrical Power & Energy Systems* 121, 106083. URL: <https://www.sciencedirect.com/science/article/pii/S0142061519337135>, doi:10.1016/j.ijepes.2020.106083.
- Nowotarski, J., Weron, R., 2018. Recent advances in electricity price forecasting: A review of probabilistic forecasting. *Renewable and Sustainable Energy Reviews* 81, 1548–1568. URL: <https://www.sciencedirect.com/science/article/pii/S1364032117308808>, doi:10.1016/j.rser.2017.05.234.
- Olivares, K.G., Challu, C., Marcjasz, G., Weron, R., Dubrawski, A., 2023. Neural basis expansion analysis with exogenous variables: Forecasting electricity prices with NBEATSx. *International Journal of Forecasting* 39, 884–900. URL: <https://www.sciencedirect.com/science/article/pii/S0169207022000413>, doi:10.1016/j.ijforecast.2022.03.001.
- O'Connor, C., Bahloul, M., Prestwich, S., Visentin, A., 2025. A Review of Electricity Price Forecasting Models in the Day-Ahead, Intra-Day, and Balancing Markets. *Energies* 18, 3097. URL: <https://www.mdpi.com/1996-1073/18/12/3097>, doi:10.3390/en18123097.
- Pelagatti, M., 2013. Supply Function Prediction in Electricity Auctions, in: Grigoletto, M., Lisi, F., Petrone, S. (Eds.), *Complex Models and Computational Methods in Statistics*, Springer Milan, Milano. pp. 203–213. URL: https://link.springer.com/10.1007/978-88-470-2871-5_16, doi:10.1007/978-88-470-2871-5_16. series Title: Contributions to Statistics.

- Petropoulos, F., Apiletti, D., Assimakopoulos, V., Babai, M.Z., Barrow, D.K., Ben Taieb, S., Bergmeir, C., Bessa, R.J., Bijak, J., Boylan, J.E., Browell, J., Carnevale, C., Castle, J.L., Cirillo, P., Clements, M.P., Cordeiro, C., Cyrino Oliveira, F.L., De Baets, S., Dokumentov, A., Ellison, J., Fiszeder, P., Franses, P.H., Frazier, D.T., Gilliland, M., Gönül, M.S., Goodwin, P., Grossi, L., Grushka-Cockayne, Y., Guidolin, M., Guidolin, M., Gunter, U., Guo, X., Guseo, R., Harvey, N., Hendry, D.F., Hollyman, R., Januschowski, T., Jeon, J., Jose, V.R.R., Kang, Y., Koehler, A.B., Kolassa, S., Kourentzes, N., Leva, S., Li, F., Litsiou, K., Makridakis, S., Martin, G.M., Martinez, A.B., Meeran, S., Modis, T., Nikolopoulos, K., Önkal, D., Paccagnini, A., Panagiotelis, A., Panapakidis, I., Pavía, J.M., Pedio, M., Pedregal, D.J., Pinson, P., Ramos, P., Rapach, D.E., Reade, J.J., Rostami-Tabar, B., Rubaszek, M., Sermpinis, G., Shang, H.L., Spiliotis, E., Syntetos, A.A., Talagala, P.D., Talagala, T.S., Tashman, L., Thomakos, D., Thorarindottir, T., Todini, E., Trapero Arenas, J.R., Wang, X., Winkler, R.L., Yusupova, A., Ziel, F., 2022. Forecasting: theory and practice. *International Journal of Forecasting* 38, 705–871. URL: <https://www.sciencedirect.com/science/article/pii/S0169207021001758>, doi:10.1016/j.ijforecast.2021.11.001.
- Ramsay, J.O., Silverman, B.W., 2005. *Functional Data Analysis*. Springer Series in Statistics, Springer, New York, NY. URL: <http://link.springer.com/10.1007/b98888>, doi:10.1007/b98888.
- Satopaa, V., Albrecht, J., Irwin, D., Raghavan, B., 2011. Finding a "Knee" in a Haystack: Detecting Knee Points in System Behavior, in: 2011 31st International Conference on Distributed Computing Systems Workshops, IEEE, Minneapolis, MN, USA. pp. 166–171. URL: <http://ieeexplore.ieee.org/document/5961514/>, doi:10.1109/ICDCSW.2011.20.
- Shah, I., Lisi, F., 2020. Forecasting of electricity price through a functional prediction of sale and purchase curves. *Journal of Forecasting* 39, 242–259. URL: <https://onlinelibrary.wiley.com/doi/abs/10.1002/for.2624>, doi:10.1002/for.2624. *eprint*: <https://onlinelibrary.wiley.com/doi/pdf/10.1002/for.2624>.
- Shang, H.L., 2013. Functional time series approach for forecasting very short-term electricity demand. *Journal of Applied Statistics* 40, 152–168. URL: <https://doi.org/10.1080/02664763.2012.740619>,

- doi:10.1080/02664763.2012.740619. publisher: Taylor & Francis
_eprint: <https://doi.org/10.1080/02664763.2012.740619>.
- Sinha, N., Lucheroni, C., 2025. Demand and supply curve forecasting using a monotonic autoencoder for short-term day-ahead electricity market bid curves. *Applied Energy* 397, 126262. URL: <https://www.sciencedirect.com/science/article/pii/S0306261925009924>, doi:10.1016/j.apenergy.2025.126262.
- Soloviova, M., Vargiolu, T., 2021. Efficient representation of supply and demand curves on day-ahead electricity markets. *The Journal of Energy Markets* URL: <https://www.risk.net/journal-of-energy-markets/7808701/efficient-representation-of-supply-and-demand-curves-on-day-ahead-electricity-markets>, doi:10.21314/JEM.2020.218.
- Tang, Q., Guo, H., Zheng, K., Chen, Q., 2024. Forecasting individual bids in real electricity markets through machine learning framework. *Applied Energy* 363, 123053. URL: <https://www.sciencedirect.com/science/article/pii/S0306261924004367>, doi:10.1016/j.apenergy.2024.123053.
- Teh, Y.W., 2011. Dirichlet Process, in: Sammut, C., Webb, G.I. (Eds.), *Encyclopedia of Machine Learning*. Springer US, Boston, MA, pp. 280–287. URL: https://link.springer.com/10.1007/978-0-387-30164-8_219, doi:10.1007/978-0-387-30164-8_219.
- Tibshirani, R., 1996. Regression Shrinkage and Selection Via the Lasso. *Journal of the Royal Statistical Society: Series B (Methodological)* 58, 267–288. URL: <https://doi.org/10.1111/j.2517-6161.1996.tb02080.x>, doi:10.1111/j.2517-6161.1996.tb02080.x.
- Uniejewski, B., 2024. Regularization for electricity price forecasting. *Operations Research and Decisions* 34. URL: https://ord.pwr.edu.pl/assets/papers_archive/ord2024vol134no3_14.pdf, doi:10.37190/ord240314.
- Uniejewski, B., Nowotarski, J., Weron, R., 2016. Automated Variable Selection and Shrinkage for Day-Ahead Electricity Price Forecasting. *Energies* 9, 621. URL: <https://www.mdpi.com/1996-1073/9/8/621>,

doi:10.3390/en9080621. number: 8 Publisher: Multidisciplinary Digital Publishing Institute.

Vivó, G., Alonso, A.M., 2024. Prediction of Intraday Electricity Supply Curves. *Applied Sciences* 14, 10663. URL: <https://www.mdpi.com/2076-3417/14/22/10663>, doi:10.3390/app142210663.

Weron, R., 2014. Electricity price forecasting: A review of the state-of-the-art with a look into the future. *International Journal of Forecasting* 30, 1030–1081. URL: <https://www.sciencedirect.com/science/article/pii/S0169207014001083>, doi:10.1016/j.ijforecast.2014.08.008.

Yıldırım, S., Khalafi, M., Güzel, T., Satık, H., Yılmaz, M., 2023. Supply Curves in Electricity Markets: A Framework for Dynamic Modeling and Monte Carlo Forecasting. *IEEE Transactions on Power Systems* 38, 3056–3069. URL: <https://ieeexplore.ieee.org/document/9899762>, doi:10.1109/TPWRS.2022.3208765. conference Name: IEEE Transactions on Power Systems.

Ziel, F., 2016. Forecasting Electricity Spot Prices Using Lasso: On Capturing the Autoregressive Intraday Structure. *IEEE Transactions on Power Systems* 31, 4977–4987. URL: <https://ieeexplore.ieee.org/document/7398175>, doi:10.1109/TPWRS.2016.2521545. conference Name: IEEE Transactions on Power Systems.

Ziel, F., Steinert, R., 2016. Electricity price forecasting using sale and purchase curves: The X-Model. *Energy Economics* 59, 435–454. URL: <https://www.sciencedirect.com/science/article/pii/S0140988316302080>, doi:10.1016/j.eneco.2016.08.008.

Ziel, F., Weron, R., 2018. Day-ahead electricity price forecasting with high-dimensional structures: Univariate vs. multivariate modeling frameworks. *Energy Economics* 70, 396–420. URL: <https://www.sciencedirect.com/science/article/pii/S014098831730436X>, doi:10.1016/j.eneco.2017.12.016.

Appendix A. Example of curves and clearing price prediction

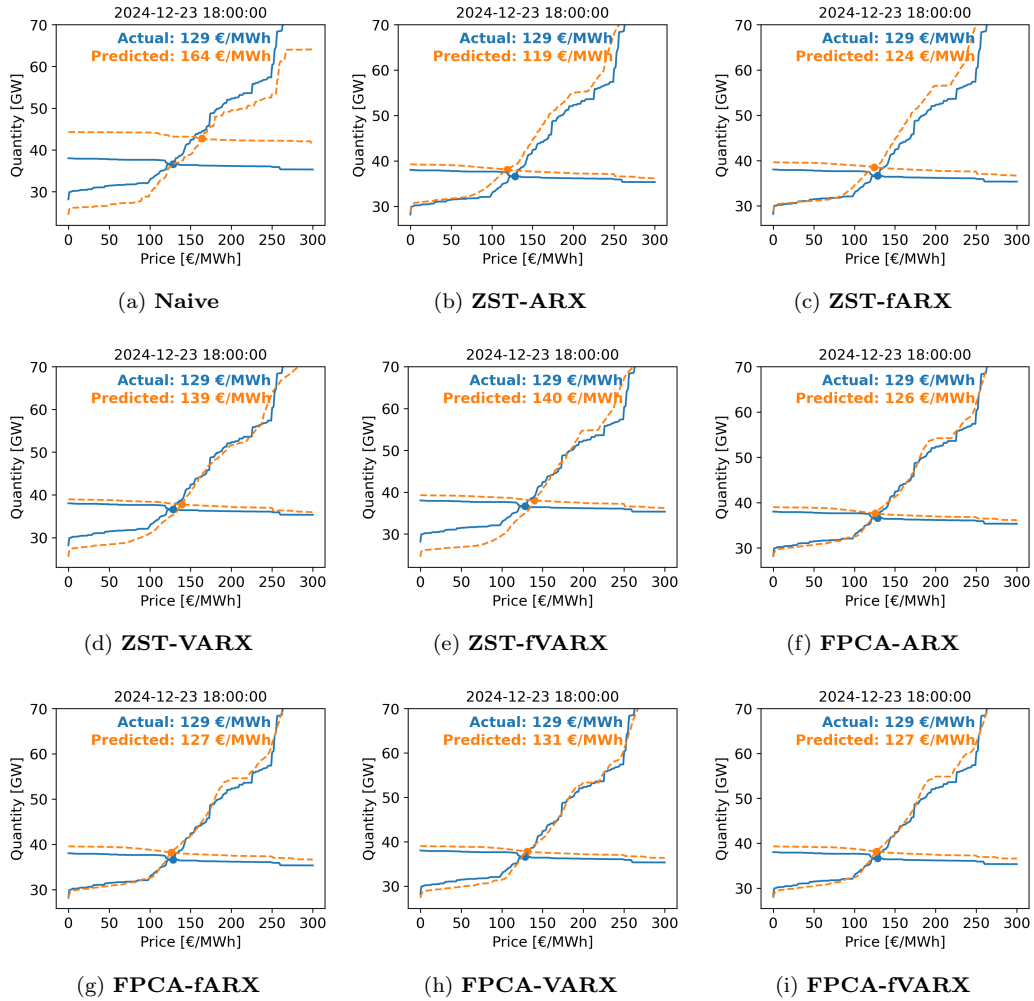


Figure A.13: Curves and clearing price predictions for the 18:00-19:00 interval of December 23rd, 2024.

Appendix B. Reliability and resolution of probabilistic forecasts

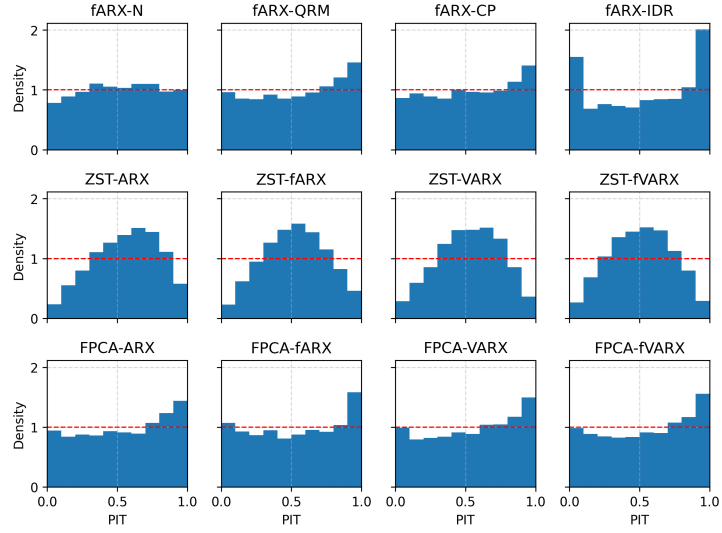


Figure B.14: Probability Integral Transform (PIT) histograms. The horizontal dashed red line corresponds to a perfect distribution fit.

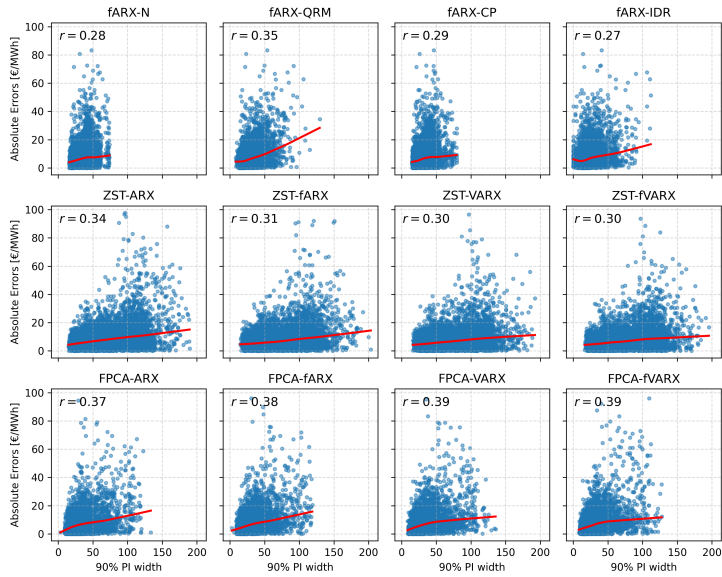


Figure B.15: Scatter plots of 90% prediction interval widths versus absolute clearing price forecasting errors for all evaluated models. The red trend line is computed using LOWESS (Cleveland, 1979) and the Spearman's correlation coefficient r is reported.